ANESTHESIOLOGY®

Clinical Electroencephalography for Anesthesiologists and Intensivists: Part 2—Physiologic Signatures and Active Management

Christian S. Guay, M.D., Uday Agrawal, M.D., Bryan Tseng, B.A., Sebastian Gallo, M.Sc., David R. Schreier, M.D., Ph.D., Emery N. Brown, M.D., Ph.D.

ANESTHESIOLOGY 2025; 143:1595–618

ABSTRACT

The electroencephalogram (EEG) offers physicians a window into their patients' neurologic and broader physiologic states. Frontal EEG interpretation is emerging as a core competency for anesthesiologists and intensivists. Part 1 of this series reviewed the basics of frontal EEG, including relevant biophysics, neuroanatomy, and anesthetic-mediated frontal EEG signatures of sedation and unconsciousness. In part 2, the authors outline a set of physiologic signatures that integrate the basics of EEG interpretation presented in part 1 with the systemic pathophysiology commonly seen in critical illness. They organize these signatures into a systematic framework to facilitate use of frontal EEG monitoring in the active management of critically ill patients. Finally, the authors use case examples to illustrate how the signatures and framework can guide patient-specific management.

(ANESTHESIOLOGY 2025; 143:1595–618)

Anesthesiologists and intensivists rely on real-time physiologic monitoring to supplement the physical examination and guide vital management decisions in critically ill patients. Hemodynamic management integrates information from the electrocardiogram, echocardiogram, and various pressure waveforms such as arterial blood pressure, central venous pressure, and pulmonary artery pressure. Respiratory management integrates information from pulse oximetry, gas analysis, and ventilator settings and measurements. Similarly, frontal electroencephalography (EEG) can supplement the neurologic examination to more accurately characterize states of sedation and unconsciousness, and guide management for the critically ill patient.

Although frontal EEG has been used for decades to titrate anesthetics during surgery, clinical use of the EEG in the intensive care unit (ICU) has been mostly limited to full scalp montages, focusing primarily on neurologic diagnoses (*e.g.*, ictal–interictal state, metabolic–toxic pattern, localized structural changes), therapeutic management (*e.g.*, status epilepticus), and recovery prognostication (*e.g.*, hypoxic brain

This article is featured in "This Month in ANESTHESIOLOGY," page A1. This article is accompanied by an editorial on p. 1446. Part of the work presented in this article has been presented (by Dr. Guay) at the 30th Annual Meeting of the Japanese Society of Cardiovascular Anesthesiologists in Yokohama, Japan, September 20, 2025.

Submitted for publication October 7, 2024. Accepted for publication July 21, 2025.

Christian S. Guay, M.D.: Department of Anesthesiology, Perioperative & Pain Medicine, University of Utah, Salt Lake City, Utah; Department of Anesthesia, Critical Care and Pain Medicine, Massachusetts General Hospital, Harvard Medical School, Boston, Massachusetts; Picower Institute for Learning & Memory, Massachusetts Institute of Technology, Cambridge, Massachusetts.

Uday Agrawal, M.D.: Department of Anesthesia, Critical Care and Pain Medicine, Massachusetts General Hospital, Harvard Medical School; Boston, Massachusetts; Department of Anesthesia, Critical Care and Pain Medicine, Massachusetts General Hospital, Harvard Medical School, Boston, Massachusetts.

Bryan Tseng, B.A.: Picower Institute for Learning & Memory, Massachusetts Institute of Technology, Cambridge, Massachusetts; Department of Biomedical Engineering, Johns Hopkins University, Baltimore, Maryland.

Sebastian Gallo, M.Sc.: Picower Institute for Learning & Memory, Massachusetts Institute of Technology, Cambridge, Massachusetts.

David R. Schreier, M.D., Ph.D.: Department of Anesthesia, Critical Care and Pain Medicine, Massachusetts General Hospital, Harvard Medical School, Boston, Massachusetts; Center for Neurotechnology and Neurorecovery, Department of Neurology, Massachusetts General Hospital and Harvard Medical School, Boston, Massachusetts; Department of Neurology, Inselspital, Bern University Hospital, and University of Bern, Bern, Switzerland.

Emery N. Brown, M.D., Ph.D.: Department of Anesthesia, Critical Care and Pain Medicine, Massachusetts General Hospital, Harvard Medical School, Boston, Massachusetts; Picower Institute for Learning & Memory, Massachusetts Institute of Technology, Cambridge, Massachusetts.

 ANESTHESIOLOGY 2025; 143:1595–618. DOI: 10.1097/ALN.0000000000005739

The article processing charge was funded by the Anesthesia Research Initiative Fund, Massachusetts Institute of Technology, Cambridge, Massachusetts.

Abbreviations: **ATP**, adenosine triphosphate; **CBF**, cerebral blood flow; **CDO_2**, cerebral delivery of oxygen; **$CMRO_2$**, cerebral metabolic rate; **CPB**, cardiopulmonary bypass; **CVP**, central venous pressure; **EEG**, electroencephalography; **GABAergic**, γ-aminobutyric acid–mediated; **ICU**, intensive care unit; **IIC**, ictal–interictal continuum; **LVAD**, left ventricular assist device; **MAP**, mean arterial pressure; **RASS**, Richmond Agitation–Sedation Scale

injury, traumatic brain injury). Accumulating evidence suggests that frontal EEG monitoring in the ICU, similar to what is used in the operating room, can guide management of critically ill patients in settings other than neurocritical care. This was supported by a recent international expert panel consensus article stating that frontal EEG monitoring competencies should be required by every category of intensivist and be made an integral component of postgraduate training programs in critical care, and that new EEG learning resources specific to the ICU are needed.[1]

This article is intended to help fill the gap in EEG education for anesthesiologists and intensivists caring for critically ill patients in the operating room and ICU. We first present a set of physiologic signatures relevant during critical illness to complement the basic anesthetic signatures introduced in part 1 of this series.[2] These signatures are then organized into an active management algorithm that uses frontal EEG to guide sedation, accelerate diagnosis, and inform therapeutic decisions at the bedside. In addition to assessing the effects of anesthetics on patients' levels of unconsciousness, frontal EEG is integrated into the broader scope of critical care, accounting for the common physiologic derangements and pathologies of critical illness.

The article is also intended to facilitate communication and collaboration with neuro-specialists by improving the non–neuro-specialist's understanding of frontal EEG. Readers are referred to excellent articles reviewing full scalp EEG and its use in neurocritical care, including for prognostication of neurologic outcomes.[3–6] The article does not review the physics of the EEG or the signatures of common anesthetics. For this, we encourage the reader to revisit part 1 of this series.[2] To maximize clinical relevance for the acute care physician, this article focuses on frontal EEG signals acquired and displayed on processed EEG devices.[7]

We first define physiologic signatures of brain states as manifest in the frontal EEG. We next present a management framework for interpreting the frontal EEG in the context of critical illness. Finally, we illustrate application of the framework with three case examples.

Methods

To illustrate certain physiologic principles and the EEG-guided management algorithm, we present cases from our institution. The data were recorded following a protocol approved by the Massachusetts General Hospital Human Studies Committee, using the Sedline monitor (Masimo Corporation, USA).

The Sedline electrodes approximate positions Fp1, Fp2, F7, and F8 according to the 10-20 system, referenced to an electrode 1 cm posterior to Fpz.[8] The impedances for all channels were less than 5 kΩ. Frontal EEG data were imported into Matlab (The MathWorks Inc., USA) and Python (Python Software Foundation, USA) for analysis. Preprocessing using the *scipy.signal* package in Python included a 60-Hz infinite impulse response notch filter; a 50-Hz, second-order Butterworth low-pass filter; and a 0.5-Hz, second-order Butterworth high-pass filter. Channels were then re-referenced to a bipolar montage, and the Fp1 to F8 channel was selected for visualization. Multitaper spectra and spectrograms were computed in Matlab using the Chronux toolbox. We used 2-s windows, 0.2-s overlap between adjacent windows, and three tapers based on a time bandwidth product of 2.[9,10] We use the term *oscillations* to describe the periodic components of the raw EEG signal at different frequencies.

We display the EEG power as a function of time using color-scaled spectrograms (also referred to as density spectral arrays), using the *jet* color map in Matlab. Power is represented in decibels, defined as 10 times the log base 10 of the squared amplitude of a given EEG frequency component. EEG power can differ by orders of magnitude across frequencies. Therefore, using logarithms makes it easier to visualize the complete range of frequencies in a signal on the same scale.

Physiologic Signatures

Cortical Rhythm Abnormalities

When starting to look at frontal EEG waveforms, it can be helpful to draw some analogies with the electrocardiogram. A normal electrocardiogram waveform is characterized by periodically occurring discharges (P waves, QRS complexes, T waves), and clinicians are trained to identify deviations from this expected normal signature. Cardiac rhythm abnormalities (*e.g.*, ventricular fibrillation) and impairments in cardiac oxygen delivery (*e.g.*, ST-segment elevation) have well-described signatures on the electrocardiogram, and their identification is crucial to guide management. Similarly, cortical rhythm abnormalities and impaired cerebral oxygen delivery exhibit signatures on the EEG (fig. 1).

Periodic discharges are a common form of cortical rhythm abnormality seen during critical illness that is often on the ictal–interictal continuum (IIC).[11,12] Although a detailed description of the IIC in critical care is beyond the scope of this article, we note that the frequency of occurrence, localization, and sharpness are important features to determine the seizure risk of rhythmic and periodic patterns.[13,14] If periodic discharges or spike-wave patterns occur at a rate greater than 2.5 Hz, *i.e.*, more than 25 discharges in a 10-s window, a seizure or status epilepticus should be suspected.[4] If they occur 11 to 25 times per 10 s, then they fall into the IIC. If their occurrence is less frequent, *i.e.*, 5 to 10 times per 10 s, but the discharges look more suspicious for an epilepsy-typical signal (*e.g.*, sharpness), then they still fall within the IIC. In general, suspected seizures, status epilepticus, or new-onset cortical periodic discharges within the IIC should prompt a neurologic consultation and a full-scalp EEG to diagnose the disorder and initiate appropriate treatment.[14,15] Rapid recognition of seizures and periodic discharges requires practice reading representative examples and common artifacts. For this, readers are referred to the

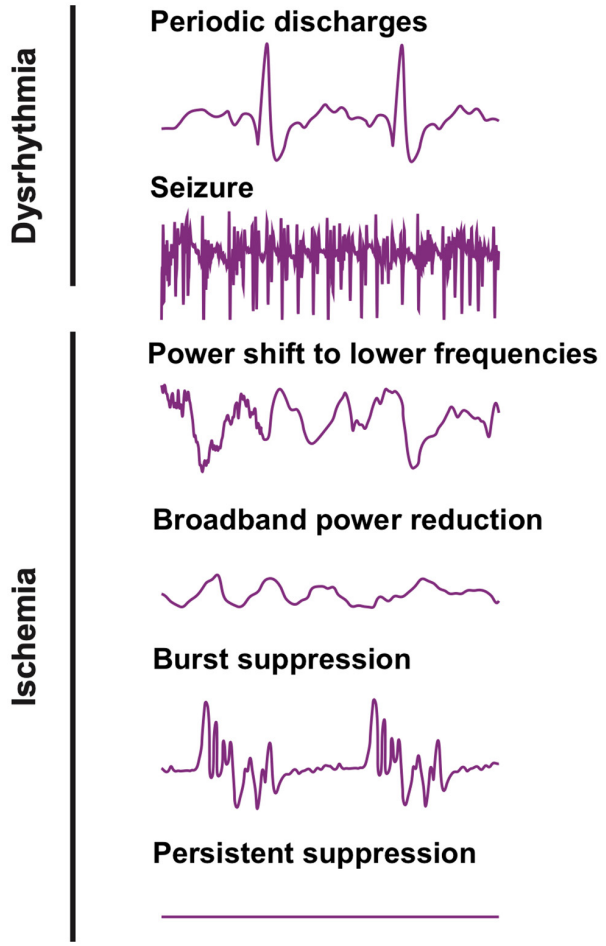

Fig. 1. Similar to electrocardiography, electroencephalography can help clinicians identify pathologic dysrhythmias and ischemia at the bedside in acute care settings. Cortical periodic discharges on the electroencephalography resemble premature ventricular contractions occurring periodically, whereas seizures resemble ventricular tachycardia or fibrillation. Signs of cerebral ischemia can also be identified in the electroencephalography. Signatures suggestive of ischemia during sedation and general anesthesia resemble those of deepening unconsciousness, such as a shift of power toward lower frequencies, broadband power reduction across all frequencies, burst suppression, and persistent suppression.

raw EEG tracings published by Sharma *et al.*[14] and the spectrograms published by Amorim *et al.*[16]

Analogous to the electrocardiogram changes related to impaired cardiac delivery of oxygen, there are EEG changes related to impaired cerebral delivery of oxygen (CDO_2). Whereas the electrocardiogram may show T-wave flattening, T-wave inversions, ST-segment depressions, and ST-segment elevations, the EEG exhibits signs of reduced neuronal activity: progressive shift of power to lower frequencies (fig. 2B *vs.* fig. 2C); power loss across all frequencies (fig. 2C *vs.* fig. 2D); and burst suppression (fig. 2E), which is characterized by intervals of low frequency and typically low-amplitude oscillations (bursts), alternating with periods of suppression (amplitude less than 10 μV).[4,17–19] Persistent cerebral ischemia and hypoxia can also cause periodic discharges and seizures during the process of progressive neuronal death (*e.g.*, after cardiac arrest), which eventually terminates in a state of electrocerebral inactivity (amplitude 2 μV or less, previously termed isoelectricity).[20–22] As we note later, impaired CDO_2 can mimic deepening pharmacologic sedation on the frontal EEG, and the two must be disentangled to guide management appropriately. Furthermore, although frontal EEG can suggest seizures or impaired CDO_2, its sensitivity for detecting these conditions is limited by the frontal EEG montage.[23,24] For example, focal temporal lobe seizures or occipital strokes may not exhibit any signs on a frontal EEG signal. Whenever neurologic pathology is suspected, frontal EEG can serve as a bedside tool but should be followed up with neurology consultation and more sensitive diagnostic testing such as full scalp EEG and appropriate imaging studies.

Beta and Gamma Oscillations. High-frequency beta (13 to 25 Hz) and gamma (greater than 25 Hz) oscillations are usually present in the normal awake brain, and typically disappear during the onset of anesthetic-mediated unconsciousness.[2,25,26] They typically re-emerge during arousal, which may occur during emergence from sedation and general anesthesia, or in response to sensory or noxious stimulation.[27,28] One notable exception is the persistence of gamma oscillations during ketamine sedation due to its complex interactions at *N*-methyl-D-aspartate receptors.[29,30] Beta oscillations may also persist in states of paradoxical excitation, a state of euphoria or dysphoria with movements during sedation at low doses of γ-aminobutyric acid–mediated (GABAergic) anesthetics such as propofol.[31]

Beta and gamma oscillations are readily identifiable in frontal EEG tracings and spectrograms as high-frequency, low-amplitude signals (fig. 2A). During sedation vacations and spontaneous breathing trials in the ICU, the emergence of beta and gamma oscillations signifies an increased rate of neuronal activity, which is expected to correlate with behavioral responsiveness on the neurologic examination.[32] A physical examination can help distinguish whether high-frequency oscillations originate from cortical activity or muscle artifacts (*e.g.*, grimacing) in the nonparalyzed patient. It is worth noting that visual assessment alone may underestimate or fail to detect subtle muscular activity. Muscle artifacts can extend to the alpha (8 to 12 Hz) and theta (4 to 8 Hz) ranges as well, *i.e.*, broadband artifact. Conversely, unexpected beta and gamma oscillations observed during neuromuscular blockade should prompt increasing the dose of anesthetic to prevent unintended awareness with recall, which can be associated with the development of posttraumatic stress disorders.[33–36] The incidence of awareness with recall during neuromuscular blockade is more common in critically ill patients who are

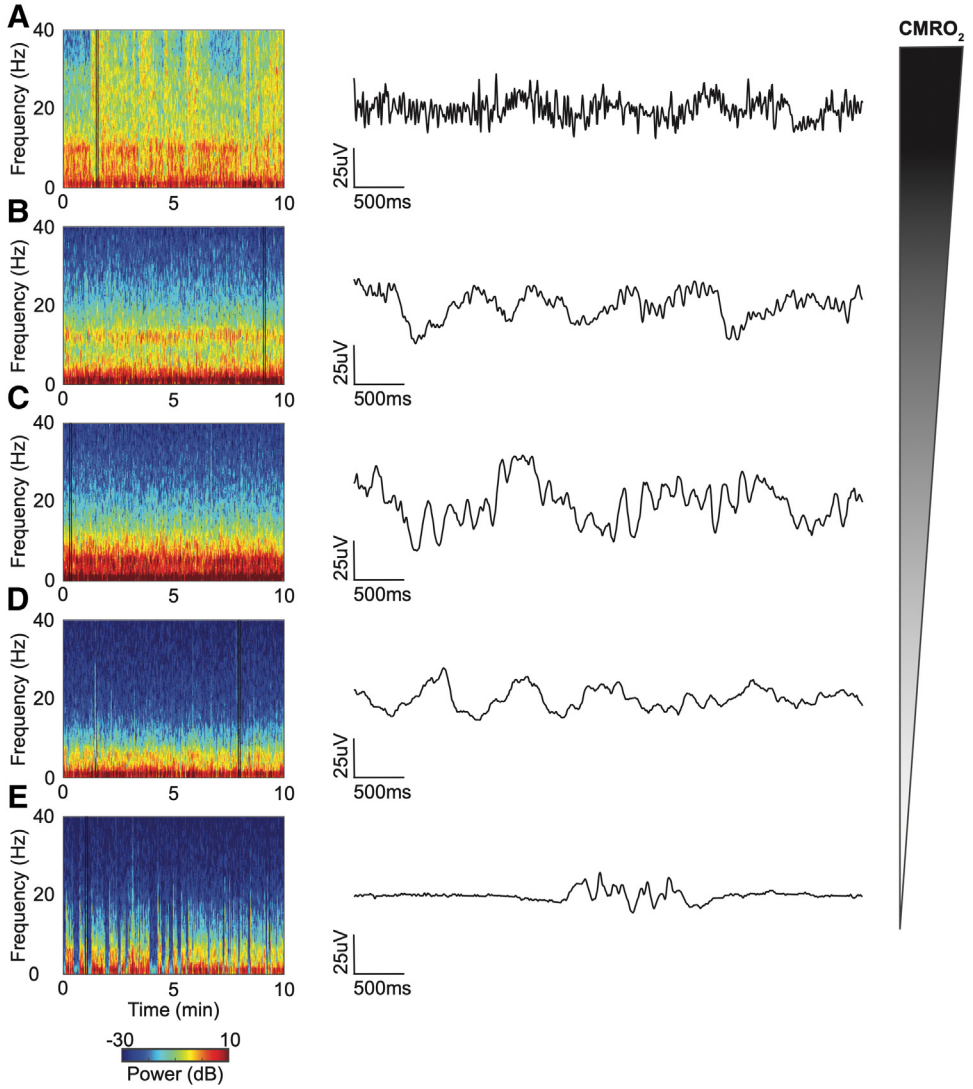

Fig. 2. Common frontal electroencephalography signatures during γ-aminobutyric acid–mediated sedation, and the associated trend in cerebral metabolic rate of oxygen ($CMRO_2$). A *black rectangle* on each spectrogram denotes the time window that is shown in the adjacent raw electroencephalography tracing. Progression from *A* through *E* during sedation or general anesthesia can indicate more profound drug-induced unconsciousness, hypothermia, or a reduction in cerebral delivery of oxygen. (*A*) Frontal electroencephalography signature of arousal and muscle artifacts, characterized by an increase in high-frequency beta (13–25 Hz) and gamma (>25 Hz) oscillations. (*B*) Frontal electroencephalography signature of sedation and unconsciousness commonly seen with γ-aminobutyric acid–mediated anesthetics (*e.g.*, propofol, sevoflurane) in nonelderly patients, characterized by slow-delta (<4 Hz) and -alpha (8–12 Hz) oscillations. (*C*) Slow-delta signature, distinguished from *B* by the lack of alpha oscillations. Theta (4–8 Hz) oscillations are also present. (*D*) Broadband power loss compared to *C*, with visibly lower slow delta amplitudes and reduction of theta power. (*E*) Burst suppression, characterized by intervals of low frequency and typically low amplitude oscillations (bursts), and periods of suppression (<10 μV).

intubated in the emergency room or ICU (1.8 to 7.4%)[37–41] compared to the operating room setting (0.07 to 0.9%).[42–44]

Alpha Oscillations. Alpha oscillations (8 to 12 Hz) were first described by Hans Berger in his seminal 1929 article, "Über das Elektrenkephalogramm des Menschen [On the Electroencephalogram of Humans]," which launched the field of electroencephalography.[45] Since then, alpha oscillations have consistently featured in the EEG literature due to their presence in wakefulness and sleep, cognition, aging, and anesthesia.[46]

In the nonsedated and well-rested human, alpha oscillations are most prominent in the occipital area during a resting, eyes-closed state.[26] The onset of behavioral unresponsiveness induced by sedatives such as propofol and dexmedetomidine correlates with decreasing occipital alpha power.[26,27,47] GABAergic sedation (*e.g.*, propofol,

sevoflurane) is further characterized by "anteriorization" of alpha oscillations whereby decreasing occipital alpha power is accompanied by a concurrent increase in frontal alpha power (fig. 2B).[48] Frontal alpha oscillations are usually accompanied by slow-delta oscillations (less than 4 Hz), completing the prototypical slow-delta–alpha signature of propofol (fig. 2B).[49] Taken together, computational models,[50,51] rodent models,[52] nonhuman primate models,[32,53] and intracranial human studies[54] suggest that propofol hyperpolarizes posterior corticothalamic networks (decreased occipital alpha) and restricts frontal corticothalamic networks to a coherent 8- to 12-Hz frequency band (increased frontal alpha).[50,51,54] Noxious stimulation in the setting of insufficient antinociception can disrupt the corticothalamic effects of GABAergic anesthetics and lead to "alpha dropout" (loss of frontal alpha power).[55,56] Furthermore, changes in amplitude modulation of frontal alpha oscillations have been shown to track unconsciousness during propofol and sevoflurane anesthesia, where deeper states of unconsciousness are associated with lower amplitude alpha oscillations.[49] Accordingly, frontal alpha oscillations have become a popular marker for tracking propofol-mediated unconsciousness using the EEG. However, patient-specific factors such as age and pathophysiologic factors such as temperature can also influence propofol-mediated frontal alpha oscillations and should be taken into consideration whenever titrating anesthetics based on frontal EEG signals. Dexmedetomidine-induced spindles resemble alpha oscillations but generally have less power, oscillate at a slightly faster frequency, are intermittent, and have more clearly defined borders in both the raw EEG tracing and spectrogram.[2,47,57,58]

In addition to serving as a marker for anesthetic states, frontal alpha oscillations have also emerged as a marker to study the aging brain and neuroinflammation. The power and peak frequency of anesthetic-induced frontal alpha oscillations evolve during the lifespan.[59–61] Alpha power first appears in sedated infants around 4 to 5 months of age and tends to peak at 6 to 8 yr old.[62–64] Alpha power declines with advancing age and may be indiscernible in some elderly patients.[59] Although these age-dependent changes are robust at a population level, frontal alpha power exhibits significant heterogeneity between patients of the same chronological age. Frontal alpha oscillations are generated by corticothalamic circuits, which also underlie cognitive functions such as attention, memory, and executive function.[65–67] Accordingly, anesthetic-induced frontal alpha power tracks cognitive functions and tends to be lower in patients with disorders of consciousness and neurocognitive disorders such as dementia and delirium.[68–72] Low frontal alpha power during GABAergic sedation and general anesthesia can also serve as a more general biomarker for frailty, higher illness severity, lower sedative requirements and increased postoperative mortality.[73–78]

In summary, patient-specific factors that are linked to weakened frontal alpha oscillations include advanced age, poor neurocognitive function, frailty, and severity of critical illness.

Slow-delta Oscillations. Large-amplitude slow (less than 1 Hz) and delta (1 to 4 Hz) oscillations in the EEG, henceforth grouped together as slow-delta (less than 4 Hz) oscillations, are ubiquitous across states of unconsciousness.[25] Seminal work throughout the twentieth century by Bremer and Steriade revealed that slow-delta oscillations constitute a default cortical rhythm.[79–81] When the cortex is isolated from ascending input by brainstem arousal centers and thalamic pacemakers, slow-delta oscillations dominate local field potentials and the EEG.[80–84] The large amplitudes of these oscillations reflect alternating "up" (depolarization and synaptic activity) and "down" (relative silence) states of cortical neurons.[79,85] Down states are prolonged (0.25- to 2-s) periods of cortical hyperpolarization and a pause in action potentials.This disrupts functional connectivity across the cortex and the capacity to sustain consciousness.[32,86] Frequency modulation of slow-delta oscillations has been shown to track GABAergic anesthetic-mediated unconsciousness (*i.e.*, deeper states of unconsciousness are associated with longer down states and slower slow-delta oscillations).[49] The restricted time window for cortical depolarization brought about by slow-delta oscillations is also associated with a depressed cerebral metabolic rate ($CMRO_2$).[25,87]

Although slow-delta oscillations are traditionally associated with states of unconsciousness, cases of behavioral responsiveness concurrent with slow-delta oscillations have been reported.This has been observed in patients with Rett syndrome, Angelman syndrome, Lennox–Gastaut syndrome, mitochondrial diseases, hepatic encephalopathy, and postoperative delirium.[88] There have also been reports of patients responding to verbal commands in the presence of anesthetic-induced slow-delta oscillations, although none of these patients reported memories of the experience.[89–91] These reports likely reflect the fact that slow-delta oscillations can be regional and that behavioral responsiveness is still possible despite a hyperpolarized and intermittently suppressed prefrontal cortex.[92] Nonetheless, the presence of slow delta oscillations remains one of the most reliable markers to track anesthetic-induced unconsciousness noninvasively.[32]

More recently, slow-delta oscillations have been found to couple electrical, hemodynamic, and cerebrospinal fluid oscillations in the human brain.[93] These brain-wide pulsations in blood volume and cerebrospinal fluid flow likely enable the clearance of cerebral metabolic byproducts, which may explain the strong association between the degradation of slow wave sleep, the accumulation of amyloid-β and tau proteins, and the onset of neurocognitive disorders.[94] Considering the emerging role of sleep disruption, neuroinflammation, and impaired cerebral metabolism in ICU-related cognitive disorders, slow-delta oscillations may represent a therapeutic target using pharmacologic

and nonpharmacologic methods to improve sleep quality, metabolite clearance, and clinical outcomes in the critically ill.[95–99]

In summary, slow-delta oscillations represent alternating up and down states in the cortex, are frequently associated with unconsciousness, and facilitate the clearance of cerebral metabolites.

Burst Suppression. Burst suppression is likely the most easily discernible rhythm on the frontal EEG (fig. 2E). It is characterized by intervals of oscillations (*i.e.*, bursts) and suppression.[4,100] Although the published threshold for EEG suppression is 10 μV, the periods of suppression during burst suppression are typically less than 5 μV.[101] In the spectrogram, periods of suppression are evident as a vertical broadband—*i.e.*, across all frequencies—signal usually colored blue or black on most clinical monitors, denoting the loss of EEG power across all frequencies. Like the down states of slow-delta oscillations, the suppression periods in burst suppression reflect a persistent lack of cortical action potentials, which may be local or global.[100] A metabolic model for burst suppression has been proposed, which posits that in states of reduced cerebral metabolism, neurons consume the available adenosine triphosphate (ATP) during a burst and then are inactive while ATP stores are sufficiently recovered to support the next burst.[102] If ATP availability is further reduced, periods of suppression become longer. If ATP availability is increased, periods of suppression become shorter. Eventually, the periods of suppression become short enough to evolve into the down states of alpha amplitude modulation and slow delta frequency modulation.[49,103]

Burst suppression can be precipitated by diverse pathophysiological states in the setting of sedation, including ischemia,[104] hypoxemia,[105] hypothermia,[103] hypoglycemia,[106] and brain injury.[107,108] Burst suppression may also intentionally be induced using GABAergic anesthetics to manage status epilepticus and critical increases in intracranial pressure.[109,110] Although propofol has been shown to inhibit mitochondrial metabolism and ATP generation in experimental models,[111–115] the precise mechanisms of propofol-induced burst suppression in clinical settings remain an area of active investigation. The mechanism likely involves both GABAergic hyperpolarization and metabolic effects.[49]

Determining the exact etiology of burst suppression in the ICU can be challenging and likely contributes to heterogeneous results in clinical outcomes studies. For example, sedation-induced burst suppression has been associated with decreased mortality after traumatic brain injury,[116] whereas unintentional burst suppression is associated with increased ICU mortality.[117,118] Although burst suppression has been associated with an increased risk of delirium,[119,120] it is more likely the patients' underlying pathophysiology that drives its effects on mortality in vulnerable populations.[118] This is exemplified in the "triple low" phenomenon whereby patients with a combination of low Bispectral Index (Medtronic, Ireland), low anesthetic concentration, and low blood pressure have an increased risk of mortality compared to patients with single or double lows.[121,122] In other words, reduced neuronal activity in the setting of systemic pathophysiology is associated with higher mortality than reduced neuronal activity in isolation.

To the best of our knowledge, experimental induction of profound hypotension, hypoxemia, or hypothermia has not been undertaken in humans without concurrent anesthesia. However, freshwater painted turtles exhibit burst suppression while hibernating in conditions of sustained anoxia and hypothermia.[123] Werner *et al.* reported that burst suppression occurred at a mean arterial pressure (MAP) of 31 ± 7 mmHg, concurrent with loss of transcranial Doppler diastolic flow, in an experimental model of hemorrhagic shock using canines anesthetized with fentanyl and nitrous oxide.[104] Although neither fentanyl nor nitrous oxide is a GABAergic anesthetic, hemorrhagic shock has been shown to increase plasma concentrations of propofol in swine, which may of itself induce burst suppression pharmacologically without invoking neuronal hypoxia.[124] In addition to this pharmacokinetic effect, shock states have also been shown to exert a pharmacodynamic effect on the brain, making it more sensitive to the effects of propofol.[125,126] More recently, a randomized controlled trial in humans demonstrated that a hemodynamic intervention aimed at restoring baseline MAP successfully terminated burst suppression more than 50% of the time in patients undergoing noncardiac surgery, without changing anesthetic dosing.[127] Whether the reported EEG findings from this trial reflect physiologic, pharmacokinetic, pharmacodynamic, or a combination of effects is still unclear. Nonetheless, new-onset burst suppression should prompt clinicians to consider a differential diagnosis that includes both anesthetic overdose and metabolic derangements.

Future work characterizing distinct burst suppression phenotypes and the underlying mechanisms will help refine our understanding of this brain state and how it can be applied as a tool and marker to improve clinical outcomes.[128–130]

Cerebral Metabolic State

The human brain's metabolic demands outscale its mass by an order of magnitude. The brain accounts for 20% of the body's oxygen consumption and only 2% of body mass.[131] This is due to the high metabolic cost incurred by neurons to support action potentials, synaptic transmission, and the maintenance of membrane potentials. These functions account for at least 75% of ATP use in the cortex.[132,133] Accordingly, neuronal ATP consumption directly correlates with average action potential rate.[133] The remaining 25% is dedicated to cellular housekeeping such as the synthesis of molecules and organelle trafficking. Considering that EEG signals fundamentally rely on these high-energy neuronal processes, *i.e.*, action potentials and postsynaptic potentials, it has long been recognized that changes in $CMRO_2$ are

hierarchically reflected in neuronal spike rates, local field potentials, and ultimately the EEG.[134,135] Simply stated, progressively decreasing $CMRO_2$ is accompanied by a shift in EEG power toward lower frequencies (*i.e.*, lower frequency of action potentials) and lower amplitudes (*i.e.*, lower number of synchronous action potentials; fig. 2).[25,32,87]

In the clinical setting, the EEG changes associated with decreasing $CMRO_2$ are most evident during the induction and reversal of hypothermia for procedures like aortic arch surgery that require periods of circulatory arrest (fig. 3). In cardiac and aortic surgery, levels of hypothermia are traditionally classified as mild (28.1° to 34°C), moderate (20.1° to 28°C), deep (14.1° to 20°C), and profound (14°C or lower).[136] After establishing cardiopulmonary bypass, the patient is systemically cooled to lower $CMRO_2$. This prolongs the safe ischemic time for the surgeon to complete the procedure in a bloodless field during circulatory arrest. As brain temperature and $CMRO_2$ decrease, there is first a shift of power toward lower frequencies, followed by broadband power reduction and then burst suppression with progressively lower amplitude bursts and longer periods of suppression until persistent suppression is achieved.[103] These EEG changes reverse during rewarming. States of profound hypothermia can decrease $CMRO_2$ by up to 90%, accounting for the reduction of action potential rate and basal metabolic rate for other cellular activities not related to synaptic transmission.[136,137]

The same sequence of frontal EEG changes observed during the induction of hypothermia has been described in cases of increasing GABAergic anesthetic concentration.[25] As propofol concentrations increase, frontal alpha power progressively decreases (*i.e.*, amplitude modulation), and the down states of slow-delta oscillations become progressively longer (*i.e.*, frequency modulation), eventually transitioning to burst suppression with ever-lengthening periods of suppression.[49] Considering the physiologic principle that neuronal energy use directly correlates with action potential frequency,[133] this EEG trajectory is accompanied by progressively decreasing $CMRO_2$. Propofol's effects on $CMRO_2$ are due to both network mechanisms (γ-aminobutyric acid agonism decreases action potential frequency and consequently decreases $CMRO_2$) and direct metabolic effects. In the latter, disruption of oxidative phosphorylation at neuronal mitochondrial membranes decreases $CMRO_2$ and consequently decreases action potential frequency.[111–115] The overlap and transition between these mechanisms has been suggested to start before the onset of burst suppression and is an area of active investigation.[49]

Decreasing CDO_2 follows a similar EEG trajectory, likely reflecting a reactive mechanism whereby the rate of action potentials, and therefore $CMRO_2$, decreases in response to declining CDO_2 caused by hypoperfusion,[104,138–140] hypoxemia,[105,141–144] or anemia[144,145] (fig. 4A). These changes are also apparent during states of prolonged hypoglycemia, reflecting the complimentary roles of oxygen and glucose in the production of neuronal ATP.[106,147] In the clinical setting, EEG signatures of reduced neuronal activity in response to low CDO_2 have been thoroughly described during carotid endarterectomies. Criteria for critical ischemic thresholds during carotid artery cross-clamping warranting consideration of a carotid shunt generally recapitulate the previously described trajectory: greater than 50% power reduction in the 8- to 15-Hz range (loss of alpha and low beta power), greater than 50% increase in slow delta power (*i.e.*, power shift toward lower frequencies), greater than 50% broadband power reduction, and EEG suppression.[19] These changes typically occur when global cerebral blood flow (CBF) falls to less than 35 to 40% (18 to 20 $ml \cdot 100\,g^{-1} \cdot min^{-1}$) of normal values (50 to 55 $ml \cdot 100\,g^{-1} \cdot min^{-1}$).[148,149] Of note, acute ischemic strokes are unlikely to cause burst suppression on the frontal EEG, although electrodes overlying affected cortical regions typically do exhibit a shift of power toward lower frequencies.[150]

Under normal circumstances, CBF is highly regulated to maintain adequate CDO_2 in response to changes in cerebral perfusion pressure, defined as the difference between MAP and the larger of intracranial pressure or central venous pressure (CVP), the partial pressures of oxygen and carbon dioxide, hemoglobin concentration, and temperature (fig. 4B).[146,151–157] However, autoregulation of CBF is disrupted in many critically ill patients and shows substantial interindividual variability.[158–160] Lower MAP limits for cerebral autoregulation range from 40 to 90 mmHg in adults, complicating precise assessment of CDO_2.[155] Furthermore, decreasing CBF may go unnoticed in patients with high hemoglobin concentration and oxygen saturation, which serve to maintain CDO_2 at an acceptable level despite lower flow. Conversely, anemic and hypoxemic patients will have less tolerance for reductions in CBF. CBF has also been shown to increase during seizures to maintain balance between oxygen supply and demand.[161] Severe hypo- and hypercapnia may also result in reduced neuronal activity *via* impairments in CBF and direct anesthetic effect,[162–165] respectively. Ultimately, the exact values of CDO_2 and $CMRO_2$ are less important than ensuring their balance, which is reflected in the electrical activity of the brain and resulting EEG signals. In this way, the frontal EEG can be used as a marker for end-organ perfusion. Unexpected shifts of frontal EEG power to lower frequencies, broadband power decreases, or the appearance of burst suppression should alert clinicians of a possible imbalance in CDO_2 and $CMRO_2$ and prompt a search for underlying causes and confounding factors such as hypothermia, hypoglycemia, and oversedation.

Behavioral State of Arousal

A focused neurologic examination assessing brainstem function and states of arousal can help inform expected drug-induced frontal EEG signatures.[166] A progressive loss of brainstem reflexes (*e.g.*, pupillary light reflex, corneal

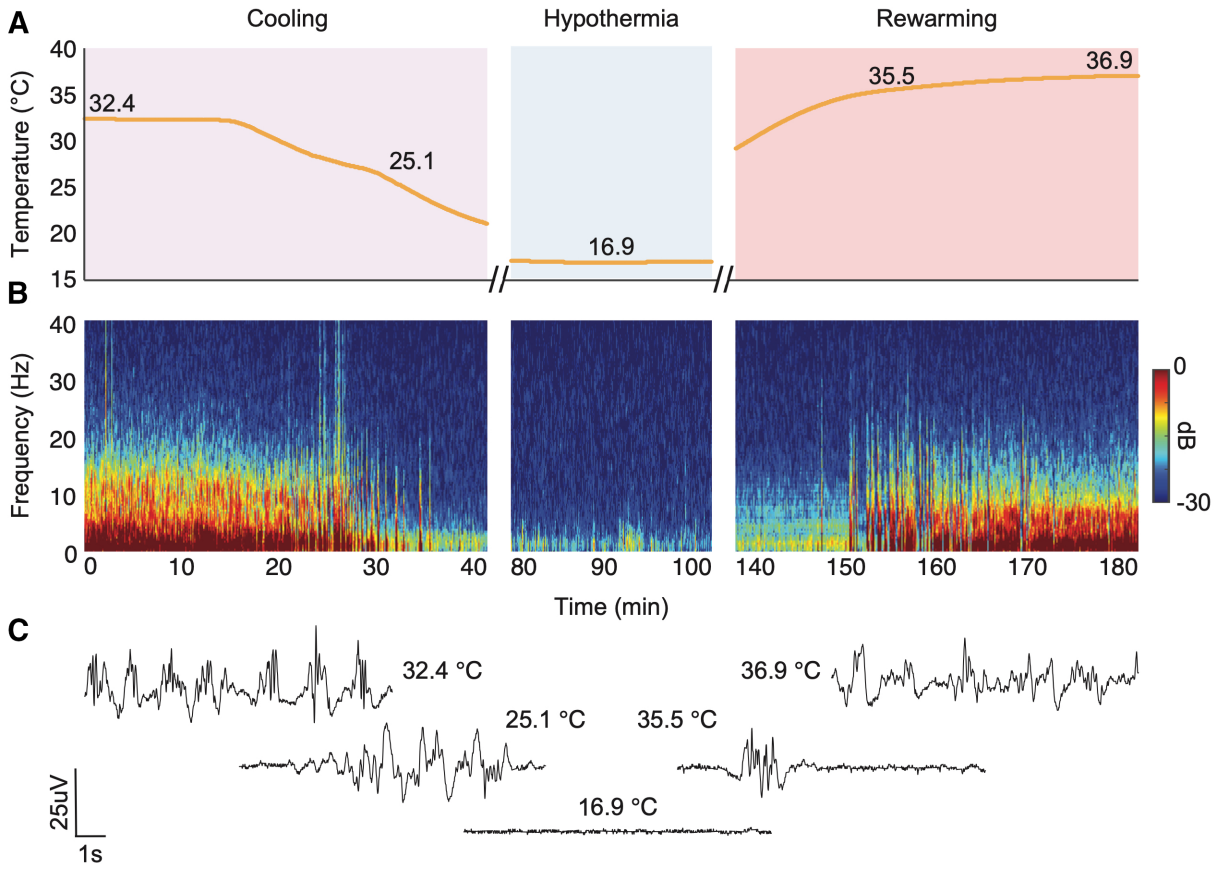

Fig. 3. Effects of progressive hypothermia and decreasing cerebral metabolic rate on the frontal electroencephalography. (*A*) Nasopharyngeal temperature time course of a patient who is cooled to induce deep hypothermia for aortic arch surgery, and subsequently rewarmed. (*B*) Spectrogram showing frontal electroencephalography correlates of the cooling, deep hypothermia and rewarming periods. (*C*) Electroencephalography tracings of different levels of hypothermia. As temperature and cerebral metabolic rate decrease, frontal electroencephalography power shifts toward lower frequencies and then transitions to burst suppression with lengthening periods of suppression until reaching persistent suppression. These electroencephalography changes reverse during rewarming.

reflex, oculocephalic reflex, gagging, coughing) suggests deepening levels of sedation.[166] The Richmond Agitation–Sedation Scale (RASS) is commonly used in clinical settings to assess states of arousal. It ranges from −5 (unresponsive) to +4 (combative) and has been validated in adult ICUs.[167]

Sedated patients without primary neurologic pathologies who do not respond to voice or physical stimulation (RASS, −5) are expected to exhibit states of slow-delta–alpha, slow-delta, or burst suppression on the frontal EEG.[48,49] Theta oscillations (4 to 8 Hz) are also common.[168] Responses to physical (RASS, −4) and verbal (RASS, −3, −2, −1) stimuli are typically associated with the abrupt appearance of beta and gamma oscillations, with a background state of slow-delta or slow-delta–alpha.[27,28] With the advent of "nonsedation" in the ICU, patients may also exhibit states of natural sleep, which are readily discernible on the frontal EEG.[169] A detailed description of sleep architecture and the associated EEG signatures is beyond the scope of this article, and readers are referred to the thorough description and representative figures of Prerau *et al.*[170] Patients who spontaneously interact with their environments (RASS, 0, +1) tend to have sustained beta and gamma oscillations.[26] The EEG of restless and agitated patients (RASS, +2, +3, +4) is characterized by frequent movement and electromyogram artifacts in the EEG.[171]

Many patients in the ICU will exhibit fluctuating changes in state of arousal, most notably during delirium. The association of lower neuronal activity with depressed states of arousal holds true in hypoactive delirium, where a shift of power toward higher frequencies correlates with resolving delirium severity.[70,71] States of arousal also fluctuate in other forms of encephalopathy (*e.g.*, sepsis associated encephalopathy, toxic–metabolic encephalopathy), which can exhibit diverse EEG phenotypes including a shift of power toward lower frequencies, burst suppression, triphasic periodic discharges, and seizures.[172,173] Patients with a predominantly slow-delta signature tend to exhibit the characteristics of hypoactive delirium, whereas burst suppression,

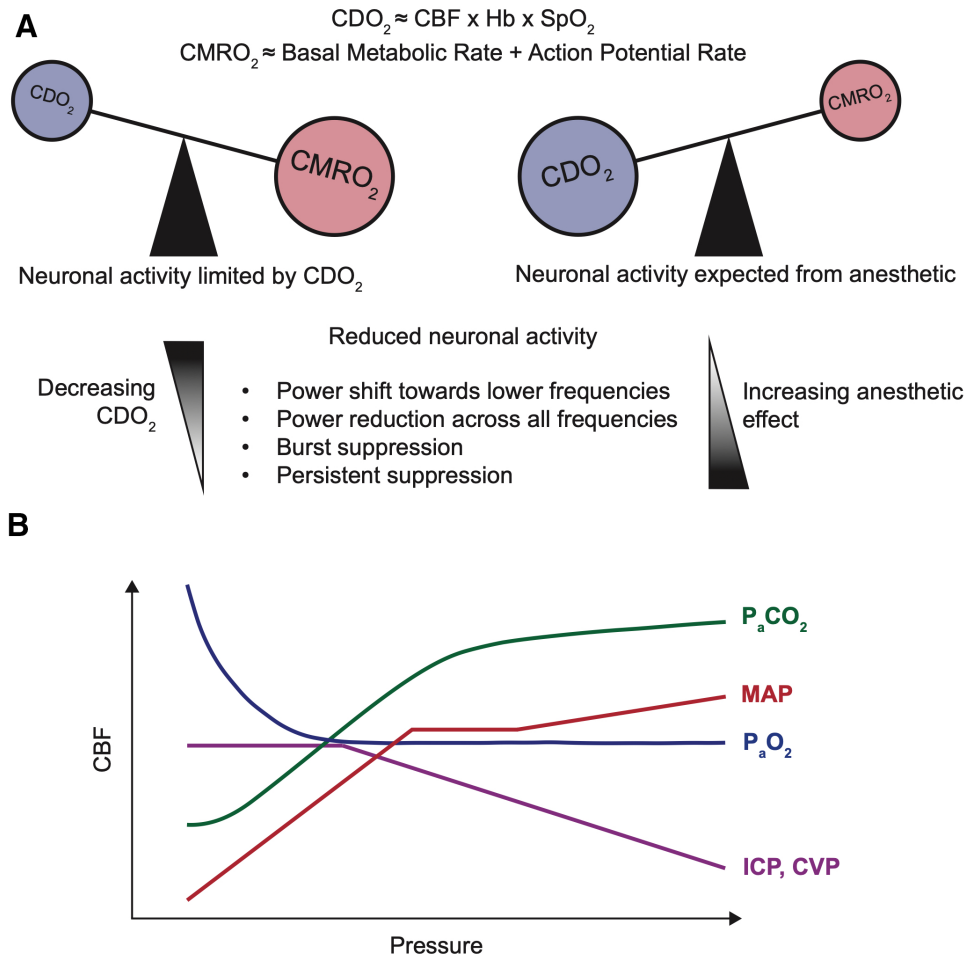

Fig. 4. Balancing the cerebral supply and demand for oxygen. (*A*) Cerebral delivery of oxygen (CDO_2) is proportional to cerebral blood flow (CBF), hemoglobin concentration (Hb) and oxygen saturation (Spo_2). Cerebral metabolic rate of oxygen ($CMRO_2$) is proportional to basal metabolic rate and action potential rate. When $CMRO_2$ persistently outweighs CDO_2 during sedation or general anesthesia, frontal electroencephalography signatures will mimic the reduced neuronal activity trajectories of progressive hypothermia or increasing γ-aminobutyric acid–mediated anesthetic effects. (*B*) Cerebral autoregulation helps maintain balance between CDO_2 and $CMRO_2$ by altering CBF in response to changes in vital parameters such as mean arterial pressure (MAP), partial pressure of oxygen (PaO_2), and partial pressure of carbon dioxide ($PaCO_2$). Increases in intracranial pressure (ICP) and central venous pressure (CVP) can impair CBF by reducing cerebral perfusion pressure. CBF can also be compromised by decreasing $PaCO_2$ and decreasing MAP.

periodic discharges, and nonconvulsive seizures typically represent more severe brain injury.[174,175]

Management Framework

By combining knowledge of the common anesthetic signatures reviewed in part 1 with the physiologic signatures of part 2, clinicians can integrate frontal EEG into management of the critically ill patient (fig. 5).

The first step is to set expectations for the patient's EEG based on contextual clinical information (fig. 5, top). Variables to consider when setting expectations should include the behavioral state of arousal, anesthetic infusions, age, comorbidities, and physiologic parameters as described in previous sections. For example, a 40-yr-old otherwise healthy woman who is sedated with 50 mcg · kg^{-1} · min^{-1} propofol after elective cardiac surgery, has stable vital signs, and opens her eyes to voice would be expected to exhibit a slow-delta–alpha signature (fig. 2B) with intermittent beta and gamma oscillations in response to verbal commands (fig. 2A). Conversely, a 78-yr-old patient who is sedated with 20 mcg · kg^{-1} · min^{-1} propofol after being intubated for hypoxemic respiratory failure, is being resuscitated for septic shock, and does not respond to verbal or physical stimuli would be expected to exhibit a slow-delta (fig. 2, C and D), burst suppression (fig. 2E), or persistent suppression pattern.

After assessing the patient and setting expectations for frontal EEG signatures, data quality should be optimized.

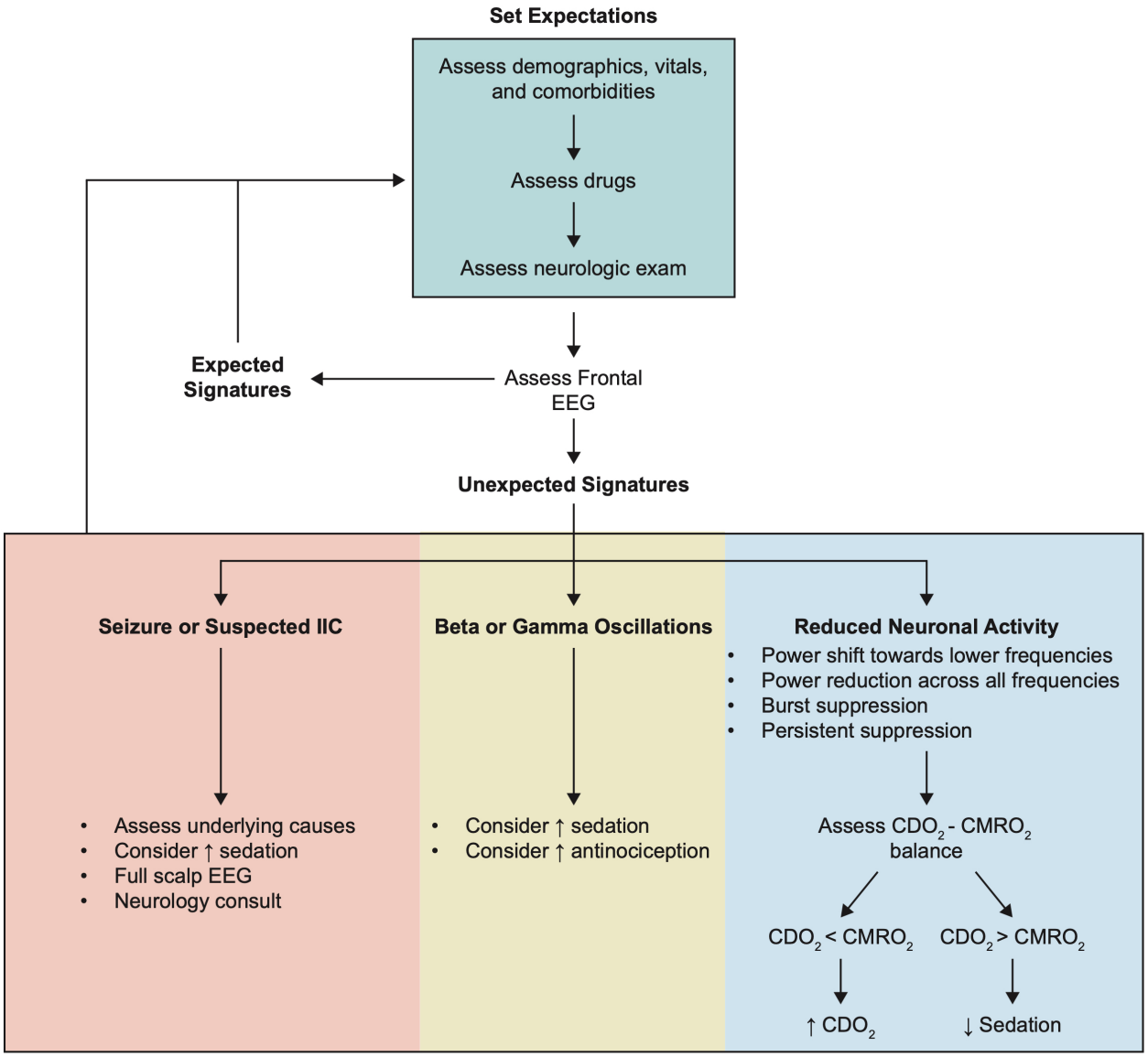

Fig. 5. Framework for electroencephalography (EEG)–guided management of the critically ill patient. The first step in the management paradigm is to assess the patient and set expectations for a frontal EEG signature (*top*). Factors to consider when setting expectations are the patient's age, vital signs, comorbidities, sedative infusions, and neurologic examination. If the patient is medically stable, has the desired state of behavioral sedation, and is displaying the expected EEG signature, no changes in management are required, and EEG monitoring can continue. If the patient is exhibiting unexpected EEG signatures, changes in management should be considered (*bottom*). Signs of seizures or the ictal–interictal continuum (IIC) should prompt a search for underlying causes, full scalp EEG, neurology consultation, and consideration of increasing sedation and administering antiseizure medications. An EEG characterized by unexpected beta (13–25 Hz) or gamma (>25 Hz) oscillations (*e.g.*, during neuromuscular blockade) suggests neurologic arousal and should prompt consideration of increasing sedation and/or antinociception to achieve the desired brain state. Patients with unexpected signs of reduced neuronal activity should first be assessed for an imbalance between cerebral delivery of oxygen (CDO_2) and cerebral metabolic rate ($CMRO_2$). If these EEG signatures persist after optimizing cerebral oxygen supply and demand, gradual lightening of sedation should proceed until expected sedative signatures are achieved. Confounding factors such as hypothermia, hypoglycemia, and severe hypercapnia should also be considered. If the signatures persist in the absence of sedation, primary neurologic pathology should be investigated.

The exact procedures differ between commercially available devices but generally include minimizing electrode impedance (*e.g.*, cleaning forehead skin, ensuring adequate electrode and gel contact) and eliminating electromagnetic artifacts (*e.g.*, avoiding wire contact with nearby electrical devices and ensuring proper grounding). Furthermore, disposable frontal EEG electrodes should be replaced every 24 h or at the manufacturer-recommended

interval. Identifying physiologic artifacts originating from nonneurologic sources is also important. In general, muscle and movement artifacts are intermittent, with broadband frequencies and high amplitudes. Eye movement artifacts can be caused by blinking (short, high-amplitude signal) and rolling eye movements (lower-frequency delta-range signal with moderate amplitude). Most processed frontal EEG devices in clinical use have adopted automated algorithms to detect artifacts and either subtract them from the displayed signal or alert clinicians to their presence on the user interface screen. Frequent movement artifacts and high electromyogram power usually indicate inadequate sedation (*i.e.*, RASS, + 2, +3, +4), hyperactive delirium, or nociception. Some devices allow users to modify the amplitude (EEG tracing, microvolts) and power (spectrogram color bar, decibel) scales, which should be optimized to identify oscillations of interest. The amplitude scale of the EEG tracing should be adjusted to the lowest possible setting where there is no signal loss (*i.e.*, peaks and troughs are not cut off from the display) to optimize visualization of lower-amplitude oscillations. The power scale of the spectrogram should be adjusted to track oscillations that are most pertinent to the patient's management.

After data quality optimization and scale adjustment, both the real-time EEG tracing and spectrograms should be assessed for drug and physiologic signatures. The EEG tracing is best suited for assessment of the current brain state, whereas the spectrogram is most helpful to identify trends over time. If the behavioral state and clinical information match the observed frontal EEG signatures, *i.e.*, expectations are met, then monitoring can continue. Future changes in the frontal EEG can be used to track disease trajectories and responses to interventions. There are no guidelines for the ideal interval between frontal EEG assessments in the general ICU population. Therefore, the frequency of EEG assessments, as with other clinical monitors, should be individualized according to patient acuity. The unstable 78-yr-old patient described would likely undergo more frequent bedside reassessments than the stable 40-yr-old. Similar to MAP and oxygen saturation measured by pulse oximetry, bedside frontal EEG can be rapidly assessed whenever a clinician enters a patient's room.

In cases where expectations do not align with the observed frontal EEG signature, further investigation and management should be pursued (fig. 5, bottom). Suspected seizure or IIC activity should prompt an assessment of underlying causes, full scalp EEG, neurology consultation, and consideration for antiseizure therapy and increased GABAergic sedation. When states of deep sedation or general anesthesia are being targeted (*e.g.*, during neuromuscular blockade), the presence of beta or gamma oscillations should prompt uptitration of sedation to mitigate the risk of awareness with recall. Ensuring adequate antinociception is also important to mitigate ascending arousal signals from noxious stimuli and to maintain a state of multimodal anesthesia.[176]

Unexpected signs of decreasing neuronal activity should prompt clinicians to consider a broad differential diagnosis (table 1). These signs include a progressive shift of power toward lower frequencies, broadband power reduction, and burst suppression with progressively longer periods of suppression. The differential diagnosis for impaired CDO_2 in a critically ill patient includes the various causes of hypoxemia, anemia, and reduced cerebral blood flow (fig. 4). All of these factors should be considered whenever a patient exhibits evolving signs of reduced neuronal activity. When available, the concurrent use of other bedside neuromonitors such as cerebral near-infrared spectroscopy and transcranial Doppler can help narrow the differential diagnosis.[177] If there are no concerns for declining CDO_2, hypothermia, hypoglycemia, severe hypercapnia, or inadequate antinociception, anesthetic infusions can be downtitrated until the desired brain state is achieved. Some patients with encephalopathy or brain injury may exhibit persistent slow-delta oscillations or burst suppression despite completely turning off the anesthetic infusions. This should be investigated further with appropriate studies. Generalized EEG suppression may also be seen after seizure termination (*i.e.*, post-ictal suppression), which typically has a higher amplitude than the suppression periods characteristic of burst suppression and only lasts a few minutes.[101]

Case Examples

We now illustrate the principles presented in previous sections with three case examples.

Case 1

A 39-yr-old woman with factor V Leiden and chronic thromboembolic pulmonary hypertension presents to

Table 1. Differential Diagnosis for Reduced Neuronal Activity, Categorized into States of Normal CDO_2 and Reduced CDO_2

Normal CDO_2	Reduced CDO_2
Anesthetic effect	Shock
Hypothermia	Intracranial hypertension
Hypoglycemia	Venous congestion
Hypercapnia	Hypoxemia
Post-ictal suppression	Hypocapnia
Nociception	Anemia
	Stroke
Primary brain injury	

Reduced CDO_2 can be caused by shock, intracranial hypertension, venous congestion, stroke, hypoxemia, hypocapnia, and anemia. In cases of normal CDO_2, causes of reduced neuronal activity include increasing anesthetic effect, hypothermia, hypoglycemia, severe hypercapnia, post-ictal suppression, and nociception. Primary brain injury may reduce neuronal activity *via* metabolic (*i.e.*, reduced CDO_2) or nonmetabolic (*i.e.*, normal CDO_2) mechanisms.

CDO_2, cerebral delivery of oxygen.

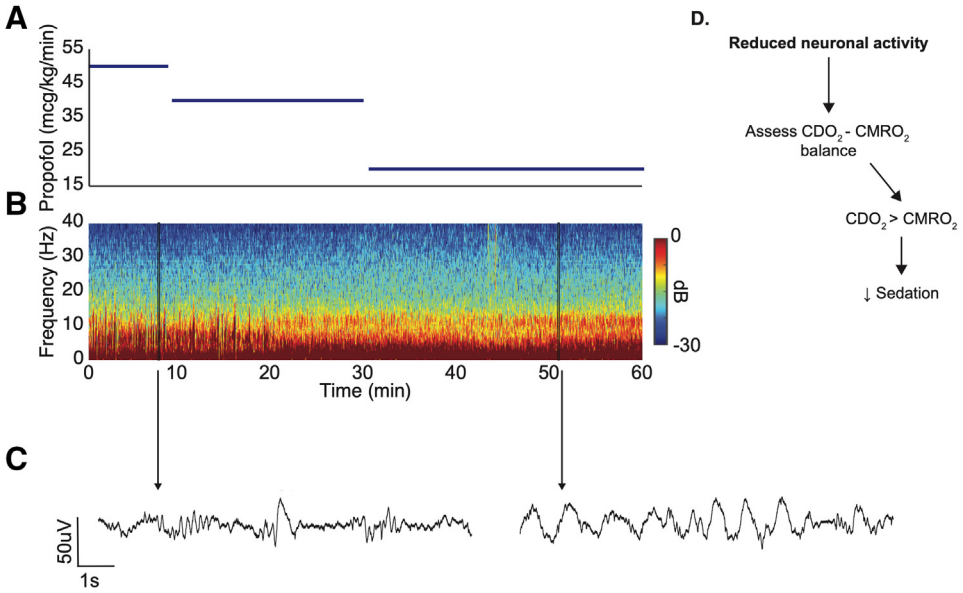

Fig. 6. Case 1a: Electroencephalography-guided propofol titration in a 39-yr-old woman with chronic thromboembolic pulmonary hypertension. This relatively young patient, sedated with propofol (50 mcg · kg^{-1} · min^{-1}) was expected to exhibit slow-delta and alpha electroencephalography oscillations. Despite normal vital signs and no concerns for an imbalance between cerebral oxygen supply and demand, she was in a state of burst suppression. The propofol infusion rate was decreased to 40 mcg · kg^{-1} · min^{-1} and then to 20 mcg · kg^{-1} · min^{-1} after which she emerged from burst suppression to the expected slow-delta–alpha electroencephalography pattern. (*A*) Propofol infusion rates. (*B*) Frontal electroencephalography spectrogram showing transition from burst suppression to slow-delta–alpha. (*C*) Frontal electroencephalography tracings corresponding to the *black rectangles* in the spectrogram, showing burst suppression at approximately 8 min in the spectrogram and then slow-delta–alpha at approximately 52 min. (*D*) Electroencephalography-guided decision path appropriate for this case. CDO_2, cerebral delivery of oxygen; $CMRO_2$, cerebral metabolic rate.

the emergency department with worsening shortness of breath and is admitted to the ICU. She is intubated due to acute hypoxemic respiratory failure, and an arterial catheter is placed to monitor blood pressure and blood gases. She remains hemodynamically stable throughout induction, intubation, and the initiation of mechanical ventilation. Laboratory testing reveals a normal hemoglobin concentration, normal glucose concentration, and blood gas analysis within normal limits. Several hours after intubation, she remains sedated with 50 mcg · kg^{-1} · min^{-1} propofol. Her neurologic examination reveals an absence of brainstem reflexes and a RASS of −5. Considering the patient's relatively young age, normothermia, propofol infusion dose, hemodynamic stability, and improved oxygenation, a slow-delta–alpha pattern is expected on her frontal EEG.

The initial examination of her frontal EEG reveals burst suppression (fig. 6). Due to the lack of clinical evidence to suggest impaired CDO_2 or other confounding causes of decreased neuronal activity, her propofol infusion is decreased to 40 and then 20 mcg · kg^{-1} · min^{-1}. Her frontal EEG then transitions to the expected slow-delta–alpha pattern, and monitoring for future unexpected signatures follows.

Two days later, the patient develops intermittent periods of changes on her frontal EEG, including loss of alpha power and burst suppression whenever her MAP is less than 70 mmHg (fig. 7). The apparent persistence of beta and gamma power during burst suppression is likely artifactual in the setting of clear burst suppression on both the EEG tracing and spectrogram. She is still sedated with 20 mcg · kg^{-1} · min^{-1} propofol and is intermittently responsive to painful stimuli. Point-of-care transthoracic echocardiography reveals worsening right ventricular systolic function, and chart review shows a gradual increase in her CVP during the past 24 h. An epinephrine infusion is initiated, which reduces her CVP and increases her MAP. Her frontal EEG then transitions from burst suppression to a stable slow-delta–alpha pattern.

This case illustrates two common scenarios in the ICU. First, the patient is oversedated and in burst suppression. EEG-guided downtitration of the propofol infusion effectively resolves the burst suppression, and the expected slow-delta–alpha signature emerges. With the slow-delta–alpha signature intact, impairments in CDO_2 can more easily be detected on the EEG during monitoring. During the course of the next 2 days, she develops right heart failure, compromising CBF, and CDO_2. Although her MAP remains above the traditionally targeted 65 mmHg, declining cardiac output and rising CVP impair cerebral perfusion pressure to the point of a CDO_2–$CMRO_2$ imbalance. It is also possible that

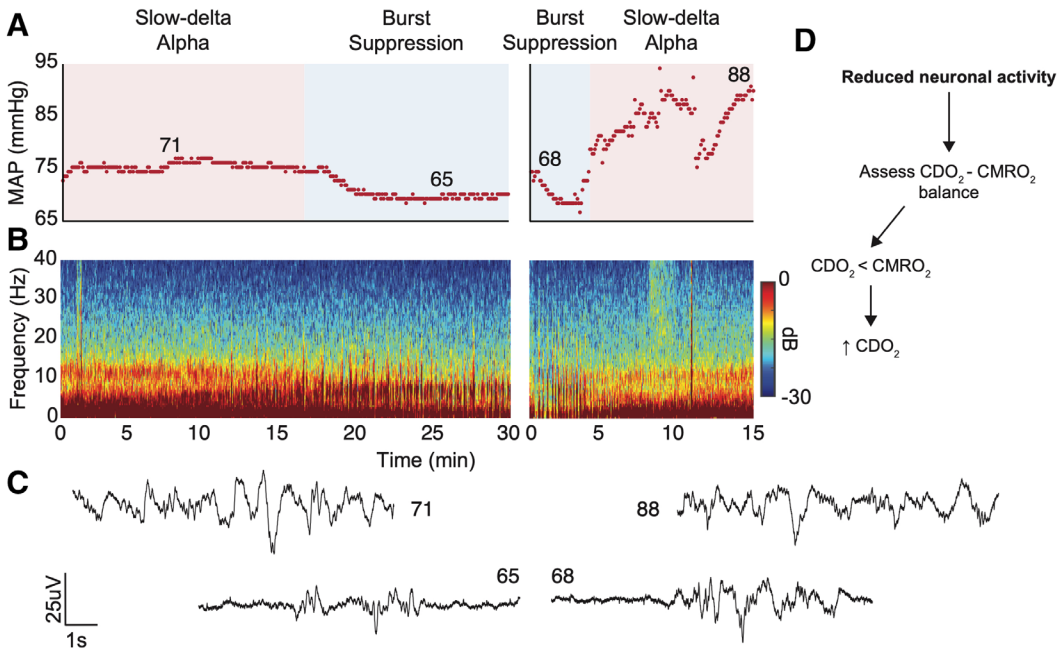

Fig. 7. Case 1b: Impaired cerebral delivery of oxygen (CDO_2) leading to burst suppression in a 39-yr-old woman with chronic thromboembolic pulmonary hypertension. The same patient described in figure 6 developed worsening right ventricular systolic function. When her mean arterial pressure (MAP) dropped to less than 70 mmHg, she transitioned from a slow-delta–alpha signature to burst suppression, despite a stable propofol infusion at 20 mcg · kg^{-1} · min^{-1}, suggesting an imbalance between CDO_2 and cerebral metabolic rate ($CMRO_2$). Elevated central venous pressure (CVP) in the setting of right ventricular failure likely increased the required MAP to maintain adequate cerebral perfusion pressure, cerebral blood flow, and CDO_2. It is also possible that burst suppression was caused by increasing propofol concentrations due to altered pharmacokinetics in the setting of reduced cardiac output. An epinephrine infusion was initiated to restore her cardiac output and mean arterial pressure, also resulting in a decreased central venous pressure. Shortly thereafter, she transitioned from burst suppression to a slow-delta signature with progressively increasing alpha power. (*A*) Time course of the patient's MAP in relation to states of slow-delta–alpha oscillations (*pink background*) or burst suppression (*blue background*). (*B*) The corresponding frontal electroencephalography spectrogram. (*C*) Frontal electroencephalography tracings and their associated MAP when recorded. (*D*) Electroencephalography-guided decision path appropriate for this case.

burst suppression was caused by increasing propofol concentrations due to altered pharmacokinetics in the setting of reduced cardiac output. Point-of-care echocardiography confirms the diagnosis, appropriate therapy is initiated, and her EEG returns to the expected slow-delta–alpha signature.

Case 2

An 89+-yr-old woman is admitted to the ICU after mitral valve replacement. In the operating room, she exhibited slow-delta oscillations with amplitudes of 30 to 40 μV during total intravenous anesthesia with propofol and intermittent fentanyl boluses. Upon arrival to the ICU, she is sedated with propofol (40 mcg · kg^{-1} · min^{-1}) and is unresponsive to external stimuli (RASS, −5). Her MAP is maintained above 65 mmHg with high doses of norepinephrine, vasopressin, and epinephrine. Based on her age and comorbidities, a slow-delta pattern is expected on her frontal EEG. Close examination of the EEG tracing reveals low EEG power, with slow-delta amplitudes in the 10- to 20-μV range, barely above the amplitude cutoff for EEG suppression (fig. 8A). Shortly after, her EEG devolves into burst suppression. Her cardiac index measured using a pulmonary artery catheter and the thermodilution method is 1.3 l · min^{-1} · m^{-2}. Point-of-care echocardiography reveals severely reduced left ventricular systolic function. A percutaneous ventricular assist device is emergently placed, which increases her cardiac index to 2.7 l · min^{-1} · m^{-2}. Reassessment of her frontal EEG reveals resolution of burst suppression and the emergence of slow-delta oscillations with amplitudes of 30 to 40 μV, as well as theta oscillations (fig. 8B).

The next day, after confirming the absence of residual neuromuscular blockade, the propofol infusion is paused to facilitate a neurologic examination. Four hours later, she remains unresponsive to voice and physical stimuli, despite stable vital signs, appropriate percutaneous ventricular assist device flow, and no other indication of clinical deterioration. Examination of her frontal EEG reveals IIC activity (triphasic periodic discharges, 10 to 15 per 10 s), prompting computed tomography examination of her head, which is

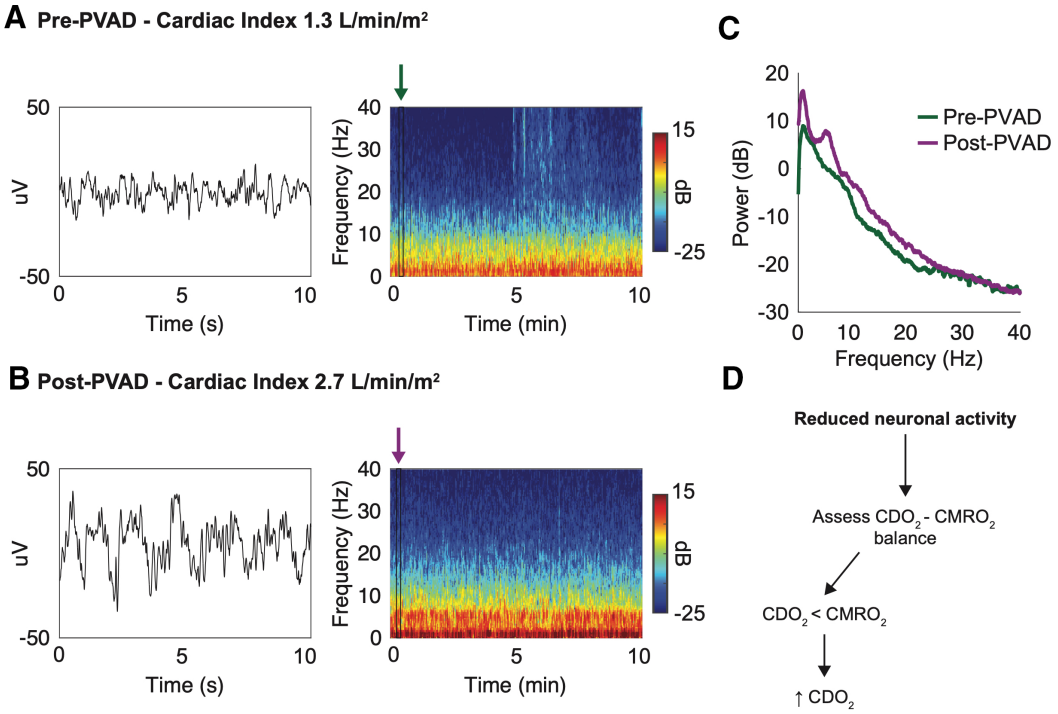

Fig. 8. Case 2a: Low cardiac output resulting in broadband power reduction in an 89+-yr-old woman after cardiac surgery. In elderly patients who have no discernable alpha power in the spectrogram, a decrease in broadband electroencephalography power can herald the onset of hemodynamic instability before burst suppression. The patient's slow-delta oscillations in the operating room were noted to have amplitudes in the 30- to 40-μV range. Upon arrival to the cardiac intensive care unit, her slow-delta amplitudes had decreased to 10 to 20 μV (*A*). Her cardiac index was measured to be 1.3 l · min^{-1} · m^{-2} using thermodilution with a pulmonary artery catheter. Shortly thereafter, her electroencephalography devolved into a burst suppression pattern. She returned to the operating room for placement of a percutaneous ventricular assist device (PVAD), which more than doubled her cardiac index (2.7 l · min^{-1} · m^{-2}). She quickly emerged from burst suppression in the operating room after initiation of PVAD flow, and upon arrival in the intensive care unit, she was noted to have recovered broadband electroencephalography power with slow-delta amplitudes back in the 30- to 40-μV range (*B*). She also exhibited theta oscillations in addition to slow-delta oscillations, indicating recovery of some faster oscillations. Unconsciousness was maintained throughout the perioperative period with 40 mcg · kg^{-1} · min^{-1} propofol, and her mean arterial pressure was maintained between 65 and 70 mmHg using vasopressors and inotropes. (*A*) Frontal electroencephalography tracing, and spectrogram during the pre-PVAD period, with a cardiac index of 1.3 l · min^{-1} · m^{-2}. (*B*) Frontal electroencephalography tracing and spectrogram during the post-PVAD period, with a cardiac index of 2.7 l · min^{-1} · m^{-2}. (*C*) Broadband electroencephalography power increase and recovery of theta oscillations after resolution of cardiogenic shock, demonstrated using median spectra computed during the time windows indicated by arrows on the spectrograms. (*D*) Electroencephalography-guided decision path appropriate for this case. CDO_2, cerebral delivery of oxygen; $CMRO_2$, cerebral metabolic rate.

unremarkable. Subsequently, a full scalp EEG reveals nonconvulsive seizure activity (fig. 9). In consultation with the neurology service, the propofol infusion is restarted, and scheduled levetiracetam is initiated. These therapies successfully suppress the seizure activity. Two days later, the patient is weaned off propofol, and she regains responsiveness to voice without any focal neurologic deficits.

This case illustrates two separate physiologic signatures. First, signs of decreased EEG activity are more subtle in elderly patients due to diminished frontal alpha power, which can be used as an early marker of clinical deterioration in younger patients. In cases such as this, broadband power reduction can serve as a warning for impending burst suppression (fig. 8C). Second, frontal EEG can help narrow the differential diagnosis for unresponsive patients during sedation vacations. In this case, it facilitated the detection of IIC activity, accelerating the diagnosis and treatment of seizures.

Case 3

A 65-yr-old man with a history of nonischemic cardiomyopathy is scheduled for cardiac surgery and insertion of a left ventricular assist device (LVAD). A right radial arterial catheter is placed before the induction of general anesthesia. Anesthetic induction, sternotomy, initiation of cardiopulmonary bypass (CPB), and insertion of the LVAD proceed uneventfully. During weaning from CPB, the frontal EEG rapidly devolves from a slow-delta–alpha pattern to burst suppression (fig. 10, A and B), despite a consistent radial artery

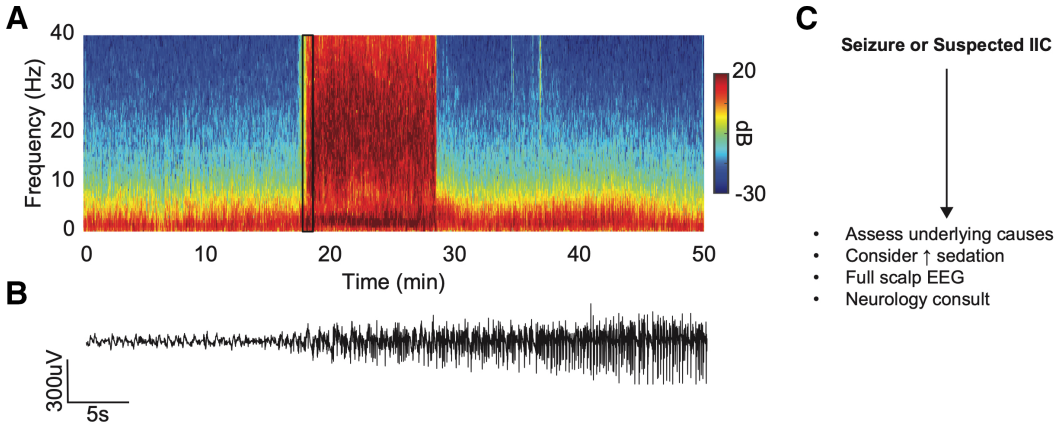

Fig. 9. Case 2b: Seizure in an 89+-yr-old woman after cardiac surgery. The same patient described in figure 8 returned to the intensive care unit in stable condition, and the next day, her propofol sedation was weaned off to facilitate neurologic examination. She remained unresponsive after 4 h, and her frontal electroencephalogram (EEG) demonstrated sharp periodic discharges. This prompted computed tomography imaging of her head without contrast, which was unremarkable, and a full montage EEG due to the concern for seizures. EEG confirmed nonconvulsive seizures, originating from her frontal lobes and generalizing across her scalp. The propofol infusion was resumed, and she was started on scheduled antiseizure medication, which effectively suppressed any further ictal–interictal continuum (IIC) or seizure activity. She regained behavioral responsiveness 2 days later without neurologic deficits. The spectrogram and raw EEG tracing *below* were derived from the Fp2 to F8 frontal channel, demonstrating seizure onset in the raw tracing and spectrogram. (*A*) Frontal EEG spectrogram showing onset and resolution of seizure activity (sustained broadband power increase visualized as a *red rectangle*). (*B*) Frontal EEG tracing showing the seizure onset. (*C*) EEG-guided decision path appropriate for this case.

MAP of 80 to 90 mmHg, albeit with no discernible pulse pressure. This observation prompts the anesthesiologist to ask the surgeon to palpate and then insert a catheter into the ascending aorta. Direct transduction of aortic pressure reveals a MAP of 35 mmHg, despite adequate LVAD flows. Full CPB is emergently reinstituted, and aortic MAP is rapidly increased using epinephrine and vasopressin. During the next minutes, burst suppression resolves, and the slow-delta–alpha signature is restored. A femoral arterial catheter is then inserted to guide hemodynamic management, and the patient is successfully weaned from CPB. The remainder of the surgery and hospital course are uneventful, and the patient is discharged with no focal neurologic deficits on postoperative day 19.

This case illustrates how the frontal EEG can serve as a marker for end-organ perfusion and alert clinicians of profound hemodynamic changes when other monitors fail. The radial artery catheter was likely compromised during CPB, resulting in an overestimation of blood pressure. Unexpected changes in the frontal EEG led to rapid diagnosis and accelerated management of a critical condition that could have otherwise resulted in devastating organ injury. In this case, the radial arterial line failed. However, similar scenarios may also arise between noninvasive blood pressure measurements or in cases of inconsistent pulse oximetry readings.

Conclusions

Integrating frontal EEG monitoring in the management of critically ill patients requires the ability to recognize basic anesthetic-induced signatures, as well as the physiologic signatures that are prevalent in this patient population. This combination allows clinicians to interpret frontal EEG signals in the full context of critical illness, and to guide management beyond titration of anesthetics. Physicians caring for the critically ill need to consider etiologies across multiple organ systems that may be driving changes in brain states.[178] Therefore, EEG education programs designed for anesthesiologists and intensivists should include physiologic signatures and representative case examples to complement traditional drug signatures and optimize the clinical utility of EEG monitoring. Future studies investigating the use of continuous frontal EEG in critically ill patients will provide new insights into the bidirectional interactions between the brain and the rest of the body. This will pave the way for specific brain state targeting to improve clinical outcomes and usher in a new era for brain health in our most vulnerable patients.

Research Support

Dr. Schreier is supported by the Swiss National Science Foundation (Bern, Switzerland; P500PM_210834). Dr. Brown is supported by the JPB Foundation (New York, New York); the Picower Institute for Learning and Memory (Cambridge, Massachusetts); George J. Elbaum (MIT '59, SM '63, PhD '67), Mimi Jensen, Diane B. Greene (MIT, SM '78), Mendel Rosenblum, Bill Swanson, annual donors to the Anesthesia Initiative Fund; and National Institutes of Health (Bethesda, Maryland) award Nos. P01 GM118269 and R01 NS123120.

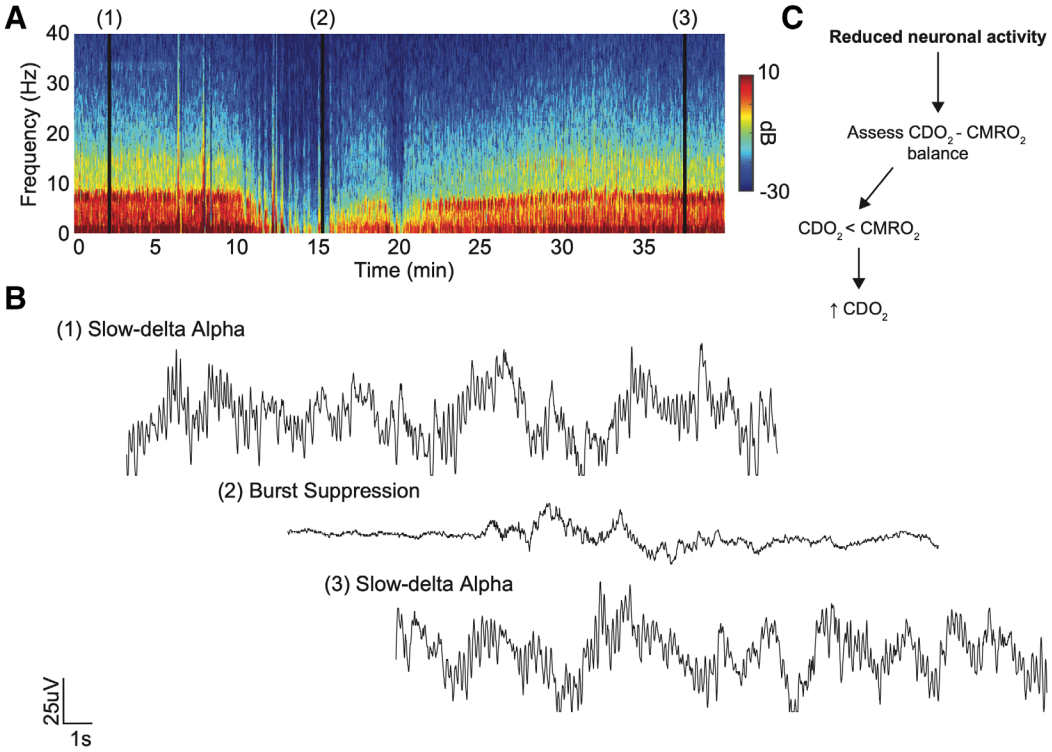

Fig. 10. Case 3: Covert hypotension leading to burst suppression in a 65-yr-old man undergoing cardiac surgery. During weaning from cardiopulmonary bypass, the frontal electroencephalogram rapidly devolves from a slow-delta–alpha pattern to burst suppression, despite a consistent radial artery mean arterial pressure of 80 to 90 mmHg. Direct transduction of aortic pressure reveals a mean arterial pressure of 35 mmHg, likely due to profound vasoplegia. Full cardiopulmonary bypass is emergently reinstituted, and aortic mean arterial pressure is rapidly increased using epinephrine and vasopressin. During the next minutes, burst suppression resolves, and the slow-delta–alpha signature is restored. (*A*) Frontal spectrogram showing the onset and resolution of burst suppression during the period of profound hypotension. (*B*) Frontal electroencephalogram tracings before (*1*), during (*2*), and after (*3*) the period of profound hypotension. (*C*) Electroencephalography-guided decision path appropriate for this case. CDO_2, cerebral delivery of oxygen; $CMRO_2$, cerebral metabolic rate.

Competing Interests

Dr. Brown is a cofounder of the start-up Pascall Systems (Cambridge, Massachusetts) that is developing systems for control of physiologic states during anesthesia, has pending patents US20200187853A1 and US20190374158A1, receives royalties from Masimo (Irvine, California) for pending patent US16373498 and issued patent US10299720, and serves on the board of directors of Humacyte, Inc. (Morrisville, North Carolina), a publicly traded company. Drs. Brown and Guay report issued patent US12059565. Dr. Guay has received travel support from Masimo to give an educational presentation at a national conference. The other authors declare no competing interests.

Correspondence

Address correspondence to Dr. Brown: Institute for Medical Engineering and Science, Picower Institute for Learning and Memory, Department of Brain and Cognitive Sciences, Massachusetts Institute of Technology, 77 Massachusetts Avenue, 46-6079, Cambridge, Massachusetts 02139 or Department of Anesthesia, Critical Care and Pain Medicine, Harvard Medical School, Massachusetts General Hospital, 55 Fruit Street, Gray-Bigelow 444, Boston, Massachusetts 02114. enb@neurostat.mit.edu

References

1. Rasulo FA, Hopkins P, Lobo FA, et al.: Processed electroencephalogram-based monitoring to guide sedation in critically ill adult patients: Recommendations from an international expert panel-based consensus. Neurocrit Care 2023; 38:296–311. doi:10.1007/s12028-022-01565-5
2. Purdon PL, Sampson A, Pavone KJ, Brown EN: Clinical electroencephalography for anesthesiologists: Part I: Background and basic signatures. Anesthesiology 2015; 123:937–60. doi:10.1097/ALN.0000000000000841
3. Herman ST, Abend NS, Bleck TP, et al.; Critical Care Continuous EEG Task Force of the American Clinical

Neurophysiology Society: Consensus statement on continuous EEG in critically ill adults and children, part I: Indications. J Clin Neurophysiol 2015; 32:87–95. doi:10.1097/WNP.0000000000000166
4. Hirsch LJ, Fong MWK, Leitinger M, et al.: American Clinical Neurophysiology Society's standardized critical care EEG terminology: 2021 version. J Clin Neurophysiol 2021; 38:1–29. doi:10.1097/WNP.0000000000000806
5. Rajajee V, Muehlschlegel S, Wartenberg KE, et al.: Guidelines for neuroprognostication in comatose adult survivors of cardiac arrest. Neurocrit Care 2023; 38:533–63. doi:10.1007/s12028-023-01688-3
6. Herman ST, Abend NS, Bleck TP, et al.; Critical Care Continuous EEG Task Force of the American Clinical Neurophysiology Society: Consensus statement on continuous EEG in critically ill adults and children, part II: Personnel, technical specifications, and clinical practice. J Clin Neurophysiol 2015; 32:96–108. doi:10.1097/WNP.0000000000000165
7. Romagnoli S, Lobo FA, Picetti E, Rasulo FA, Robba C, Matta B: Non-invasive technology for brain monitoring: Definition and meaning of the principal parameters for the International PRactice On TEChnology neuro-monitoring group (I-PROTECT). J Clin Monit Comput 2024; 38:827–45. doi:10.1007/s10877-024-01146-1
8. Jasper H: Report of the committee on methods of clinical examination in electroencephalography. Electroencephalogr Clin Neurophysiol 1958; 10:370–5
9. Bokil H, Andrews P, Kulkarni JE, Mehta S, Mitra PP: Chronux: A platform for analyzing neural signals. J Neurosci Methods 2010; 192:146–51. doi:10.1016/j.jneumeth.2010.06.020
10. Babadi B, Brown EN: A review of multitaper spectral analysis. IEEE Trans Biomed Eng 2014; 61:1555–64. doi:10.1109/TBME.2014.2311996
11. Kurtz P, Gaspard N, Wahl AS, et al.: Continuous electroencephalography in a surgical intensive care unit. Intensive Care Med 2014; 40:228–34. doi:10.1007/s00134-013-3149-8
12. Swisher CB, Shah D, Sinha SR, Husain AM: Baseline EEG pattern on continuous ICU EEG monitoring and incidence of seizures. J Clin Neurophysiol 2015; 32:147–51. doi:10.1097/WNP.0000000000000157
13. Rodriguez Ruiz A, Vlachy J, Lee JW, et al.; Critical Care EEG Monitoring Research Consortium: Association of periodic and rhythmic electroencephalographic patterns with seizures in critically ill patients. JAMA Neurol 2017; 74:181–8. doi:10.1001/jamaneurol.2016.4990.
14. Sharma S, Nunes M, Alkhachroum A: Adult critical care electroencephalography monitoring for seizures: A narrative review. Front Neurol 2022; 13:951286. doi:10.3389/fneur.2022.951286
15. Zafar SF, Subramaniam T, Osman G, Herlopian A, Struck AF: Electrographic seizures and ictal-interictal continuum (IIC) patterns in critically ill patients. Epilepsy Behav 2020; 106:107037. doi:10.1016/j.yebeh.2020.107037
16. Amorim E, Williamson CA, Moura LMVR, et al.: Performance of spectrogram-based seizure identification of adult EEGs by critical care nurses and neurophysiologists. J Clin Neurophysiol 2017; 34:359–64. doi:10.1097/WNP.0000000000000368
17. Jameson LC, Janik DJ, Sloan TB: Electrophysiologic monitoring in neurosurgery. Anesthesiol Clin 2007; 25:605–30 x. doi:10.1016/j.anclin.2007.05.004
18. Diedler J, Sykora M, Bast T, et al.: Quantitative EEG correlates of low cerebral perfusion in severe stroke. Neurocrit Care 2009; 11:210–6. doi:10.1007/s12028-009-9236-6
19. Isley MR, Edmonds HL Jr, Stecker M; American Society of Neurophysiological Monitoring: Guidelines for intraoperative neuromonitoring using raw (analog or digital waveforms) and quantitative electroencephalography: A position statement by the American Society of Neurophysiological Monitoring. J Clin Monit Comput 2009; 23:369–90. doi:10.1007/s10877-009-9191-y
20. Backman S, Westhall E, Dragancea I, et al.: Electroencephalographic characteristics of status epilepticus after cardiac arrest. Clin Neurophysiol 2017; 128:681–8. doi:10.1016/j.clinph.2017.01.002
21. Ruijter BJ, van Putten MJAM, Hofmeijer J: Generalized epileptiform discharges in postanoxic encephalopathy: Quantitative characterization in relation to outcome. Epilepsia 2015; 56:1845–54. doi:10.1111/epi.13202
22. Stecker MM, Sabau D, Sullivan L, et al.: American Clinical Neurophysiology Society guideline 6: Minimum technical standards for EEG recording in suspected cerebral death. J Clin Neurophysiol 2016; 33:324–7. doi:10.1097/WNP.0000000000000322
23. Young GB, Sharpe MD, Savard M, Al Thenayan E, Norton L, Davies-Schinkel C: Seizure detection with a commercially available bedside EEG monitor and the subhairline montage. Neurocrit Care 2009; 11:411–6. doi:10.1007/s12028-009-9248-2
24. Tanner AEJ, Särkelä MOK, Virtanen J, et al.: Application of subhairline EEG montage in intensive care unit: Comparison with full montage. J Clin Neurophysiol 2014;31:181–6.doi:10.1097/WNP.0000000000000049
25. Brown EN, Lydic R, Schiff ND: General anesthesia, sleep, and coma. N Engl J Med 2010; 363:2638–50. doi:10.1056/NEJMra0808281
26. Guay CS, Hight D, Palanca BJ: Pharmacodynamics of a stimulus-free behavioural paradigm to track conscious states during sedation with dexmedetomidine. Br J Anaesth 2023; 130:e393–4. doi:10.1016/j.bja.2022.07.024
27. Scheinin A, Kallionpää RE, Li D, et al.: Differentiating drug-related and state-related effects of dexmedetomidine and propofol on the

electroencephalogram. Anesthesiology 2018; 129:22–36. doi:10.1097/ALN.0000000000002192
28. Sleigh JW, Vacas S, Flexman AM, Talke PO: Electroencephalographic arousal patterns under dexmedetomidine sedation. Anesth Analg 2018; 127:951–9. doi:10.1213/ANE.0000000000003590
29. Adam E, Kowalski M, Akeju O, et al.: Ketamine can produce oscillatory dynamics by engaging mechanisms dependent on the kinetics of NMDA receptors. Proc Natl Acad Sci U S A 2024; 121:e2402732121. doi:10.1073/pnas.2402732121
30. Akeju O, Song AH, Hamilos AE, et al.: Electroencephalogram signatures of ketamine anesthesia-induced unconsciousness. Clin Neurophysiol 2016; 127:2414–22. doi:10.1016/j.clinph.2016.03.005
31. Gugino LD, Chabot RJ, Prichep LS, John ER, Formanek V, Aglio LS: Quantitative EEG changes associated with loss and return of consciousness in healthy adult volunteers anaesthetized with propofol or sevoflurane. Br J Anaesth 2001; 87:421–8. doi:10.1093/bja/87.3.421
32. Bastos AM, Donoghue JA, Brincat SL, et al.: Neural effects of propofol-induced unconsciousness and its reversal using thalamic stimulation. Elife 2021; 10:e60824. doi:10.7554/eLife.60824
33. Kent CD, Mashour GA, Metzger NA, Posner KL, Domino KB: Psychological impact of unexpected explicit recall of events occurring during surgery performed under sedation, regional anaesthesia, and general anaesthesia: Data from the Anesthesia Awareness Registry. Br J Anaesth 2013; 110:381–7. doi:10.1093/bja/aes386
34. Osterman JE, Hopper J, Heran WJ, Keane TM, van der Kolk BA: Awareness under anesthesia and the development of posttraumatic stress disorder. Gen Hosp Psychiatry 2001; 23:198–204. doi:10.1016/s0163-8343(01)00142-6
35. Leslie K, Chan MTV, Myles PS, Forbes A, McCulloch TJ: Posttraumatic stress disorder in aware patients from the B-aware trial. Anesth Analg 2010; 110:823–8. doi:10.1213/ANE.0b013e3181b8b6ca
36. Mashour GA, Avidan MS: Psychological trajectories after intraoperative awareness with explicit recall. Anesth Analg 2014; 119:1–3. doi:10.1213/ANE.0000000000000265
37. Moss M, Huang DT, Brower RG, et al.; National Heart, Lung, and Blood Institute PETAL Clinical Trials Network: Early neuromuscular blockade in the acute respiratory distress syndrome. N Engl J Med 2019; 380:1997–2008. doi:10.1056/NEJMoa1901686
38. Pappal RD, Roberts BW, Mohr NM, et al.: The ED-AWARENESS study: A prospective, observational cohort study of awareness with paralysis in mechanically ventilated patients admitted from the emergency department. Ann Emerg Med 2021; 77:532–44. doi:10.1016/j.annemergmed.2020.10.012
39. Fuller BM, Pappal RD, Mohr NM, et al.: Awareness with paralysis among critically ill emergency department patients: A prospective cohort study. Crit Care Med 2022; 50:1449–60. doi:10.1097/CCM.0000000000005626
40. Pappal RD, Roberts BW, Winkler W, Yaegar LH, Stephens RJ, Fuller BM: Awareness with paralysis in mechanically ventilated patients in the emergency department and ICU: A systematic review and meta-analysis. Crit Care Med 2021; 49:e304–14. doi:10.1097/CCM.0000000000004824
41. Driver BE, Prekker ME, Wagner E, et al.: Recall of awareness during paralysis among ED patients undergoing tracheal intubation. Chest 2023; 163:313–23. doi:10.1016/j.chest.2022.08.2232
42. Myles PS, Leslie K, McNeil J, Forbes A, Chan MTV: Bispectral index monitoring to prevent awareness during anaesthesia: The B-Aware randomised controlled trial. Lancet 2004; 363:1757–63. doi:10.1016/S0140-6736(04)16300-9
43. Avidan MS, Jacobsohn E, Glick D, et al.; BAG-RECALL Research Group: Prevention of intraoperative awareness in a high-risk surgical population. N Engl J Med 2011; 365:591–600. doi:10.1056/NEJMoa1100403
44. Avidan MS, Zhang L, Burnside BA, et al.: Anesthesia awareness and the Bispectral Index. N Engl J Med 2008; 358:1097–108. doi:10.1056/NEJMoa0707361
45. Berger H: Über das Elektrenkephalogramm des Menschen. Archiv f Psychiatrie 1929; 101:452–69. doi:10.1007/bf01789984
46. Quigley C: Forgotten rhythms? Revisiting the first evidence for rhythms in cognition. Eur J Neurosci 2022; 55:3266–76. doi:10.1111/ejn.15450
47. Akeju O, Pavone KJ, Westover MB, et al.: A comparison of propofol- and dexmedetomidine-induced electroencephalogram dynamics using spectral and coherence analysis. Anesthesiology 2014; 121:978–89. doi:10.1097/ALN.0000000000000419
48. Purdon PL, Pierce ET, Mukamel EA, et al.: Electroencephalogram signatures of loss and recovery of consciousness from propofol. Proc Natl Acad Sci U S A 2013; 110:E1142–51. doi:10.1073/pnas.1221180110
49. Adam E, Kwon O, Montejo KA, Brown EN: Modulatory dynamics mark the transition between anesthetic states of unconsciousness. Proc Natl Acad Sci U S A 2023; 120:e2300058120. doi:10.1073/pnas.2300058120
50. Vijayan S, Ching S, Purdon PL, Brown EN, Kopell NJ: Thalamocortical mechanisms for the anteriorization of α rhythms during propofol-induced unconsciousness. J Neurosci 2013; 33:11070–5. doi:10.1523/JNEUROSCI.5670-12.2013
51. Ching S, Cimenser A, Purdon PL, Brown EN, Kopell NJ: Thalamocortical model for a propofol-induced alpha-rhythm associated with loss of consciousness. Proc Natl Acad Sci U S A 2010; 107:22665–70. doi:10.1073/pnas.1017069108

52. Flores FJ, Hartnack KE, Fath AB, et al.: Thalamocortical synchronization during induction and emergence from propofol-induced unconsciousness. Proc Natl Acad Sci U S A 2017; 114:E6660–8. doi:10.1073/pnas.1700148114
53. Tinker JH, Sharbrough FW, Michenfelder JD: Anterior shift of the dominant EEG rhythm during anesthesia in the Java monkey: Correlation with anesthetic potency. Anesthesiology 1977; 46:252–9. doi:10.1097/00000542-197704000-00005
54. Weiner VS, Zhou DW, Kahali P, et al.: Propofol disrupts alpha dynamics in functionally distinct thalamocortical networks during loss of consciousness. Proc Natl Acad Sci U S A 2023; 120:e2207831120. doi:10.1073/pnas.2207831120
55. Hight DF, Gaskell AL, Kreuzer M, Voss LJ, García PS, Sleigh JW: Transient electroencephalographic alpha power loss during maintenance of general anaesthesia. Br J Anaesth 2019; 122:635–42. doi:10.1016/j.bja.2018.11.029
56. García PS, Kreuzer M, Hight D, Sleigh JW: Effects of noxious stimulation on the electroencephalogram during general anaesthesia: A narrative review and approach to analgesic titration. Br J Anaesth 2021; 126:445–57. doi:10.1016/j.bja.2020.10.036
57. Xi C, Sun S, Pan C, Ji F, Cui X, Li T: Different effects of propofol and dexmedetomidine sedation on electroencephalogram patterns: Wakefulness, moderate sedation, deep sedation and recovery. PLoS One 2018; 13:e0199120. doi:10.1371/journal.pone.0199120
58. Akeju O, Kim S-E, Vazquez R, et al.: Spatiotemporal dynamics of dexmedetomidine-induced electroencephalogram oscillations. PLoS One 2016; 11:e0163431. doi:10.1371/journal.pone.0163431
59. Purdon PL, Pavone KJ, Akeju O, et al.: The ageing brain: Age-dependent changes in the electroencephalogram during propofol and sevoflurane general anaesthesia. Br J Anaesth 2015; 115:i46–57. doi:10.1093/bja/aev213
60. Boncompte G, Freedman I, Qu J, et al.: Cognitive function mediates the relationship between age and anaesthesia-induced oscillatory-specific alpha power. Brain Commun 2024; 6:fcae023. doi:10.1093/braincomms/fcae023
61. Biggs D, Boncompte G, Pedemonte JC, Fuentes C, Cortinez LI: The effect of age on electroencephalogram measures of anesthesia hypnosis: A comparison of BIS, alpha power, Lempel-Ziv complexity and permutation entropy during propofol induction. Front Aging Neurosci 2022; 14:910886. doi:10.3389/fnagi.2022.910886
62. Brandt SP, Walsh EC, Cornelissen L, et al.: Case studies using the electroencephalogram to monitor anesthesia-induced brain states in children. Anesth Analg 2020; 131:1043–56. doi:10.1213/ANE.0000000000004817
63. Cornelissen L, Kim S-E, Purdon PL, Brown EN, Berde CB: Age-dependent electroencephalogram (EEG) patterns during sevoflurane general anesthesia in infants. Elife 2015; 4:e06513. doi:10.7554/eLife.06513
64. Lee JM, Akeju O, Terzakis K, et al.: A prospective study of age-dependent changes in propofol-induced electroencephalogram oscillations in children. Anesthesiology 2017; 127:293–306. doi:10.1097/ALN.0000000000001717
65. Giattino CM, Gardner JE, Sbahi FM, et al.; MADCO-PC Investigators: Intraoperative frontal alpha-band power correlates with preoperative neurocognitive function in older adults. Front Syst Neurosci 2017; 11:24. doi:10.3389/fnsys.2017.00024
66. Rossini PM, Rossi S, Babiloni C, Polich J: Clinical neurophysiology of aging brain: From normal aging to neurodegeneration. Prog Neurobiol 2007; 83:375–400. doi:10.1016/j.pneurobio.2007.07.010
67. Liu Y, Bengson J, Huang H, Mangun GR, Ding M: Top-down modulation of neural activity in anticipatory visual attention: Control mechanisms revealed by simultaneous EEG-fMRI. Cereb Cortex 2016; 26:517–29. doi:10.1093/cercor/bhu204
68. Guessous K, Touchard C, Glezerson B, et al.: Intraoperative electroencephalography alpha-band power is a better proxy for preoperative low MoCA under propofol compared with sevoflurane. Anesth Analg 2023; 137:1084–92. doi:10.1213/ANE.0000000000006422
69. Touchard C, Cartailler J, Levé C, et al.: Propofol requirement and EEG alpha band power during general anesthesia provide complementary views on preoperative cognitive decline. Front Aging Neurosci 2020; 12:593320. doi:10.3389/fnagi.2020.593320
70. Guay CS, Kafashan M, Huels ER, et al.: Postoperative delirium severity and recovery correlate with electroencephalogram spectral features. Anesth Analg 2023; 136:140–51. doi:10.1213/ane.0000000000006075
71. Palanca BJA, Guay CS: Associations between delirium and electroencephalographic markers: Notes from the field. Clin Neurophysiol 2021; 132:210–1. doi:10.1016/j.clinph.2020.10.013
72. Colombo MA, Comanducci A, Casarotto S, et al.: Beyond alpha power: EEG spatial and spectral gradients robustly stratify disorders of consciousness. Cereb Cortex 2023; 33:7193–210. doi:10.1093/cercor/bhad031
73. Shao YR, Kahali P, Houle TT, et al.: Low frontal alpha power is associated with the propensity for burst suppression: An electroencephalogram phenotype for a "vulnerable brain." Anesth Analg 2020; 131:1529–39. doi:10.1213/ANE.0000000000004781
74. Fang P-P, Zhang H-W, Hao X-X, Shang Z-X, Li J, Liu X-S: Intraoperative electroencephalogram features related to frailty in older patients: An exploratory prospective observational study. J Clin Monit Comput 2024; 38:613–21. doi:10.1007/s10877-024-01126-5

75. Kaiser HA, Hirschi T, Sleigh C, et al.: Comorbidity-dependent changes in alpha and broadband electroencephalogram power during general anaesthesia for cardiac surgery. Br J Anaesth 2020; 125:456–65. doi:10.1016/j.bja.2020.06.054
76. Kaiser HA, Hirschi T, Hartwich V, et al.: Decreasing frontal electroencephalogram alpha power and increasing sensitivity to volatile anesthetics over 3 surgeries within 7 months: A case report. A A Pract 2019; 13:274–7. doi:10.1213/XAA.0000000000001053
77. Guay CS, Bean CD, Kwon O, Brown EN: Recovery from acute respiratory distress syndrome is associated with increasing alpha power in the frontal electroencephalogram during propofol sedation: A case report. A A Pract 2023; 17:e01698. doi:10.1213/XAA.0000000000001698
78. Mather RV, Nipp RD, Balanza G, et al.: Intraoperative frontal EEG alpha power is associated with post-operative mortality and other adverse outcomes. Anesthesiology 2024; 142:500–10. doi:10.1097/aln.0000000000005315
79. Sanchez-Vives MV, Massimini M, Mattia M: Shaping the default activity pattern of the cortical network. Neuron 2017; 94:993–1001. doi:10.1016/j.neuron.2017.05.015
80. Steriade M, Nuñez A, Amzica F: Intracellular analysis of relations between the slow (< 1 Hz) neocortical oscillation and other sleep rhythms of the electroencephalogram. J Neurosci 1993; 13:3266–83. doi:10.1523/JNEUROSCI.13-08-03266.1993
81. Bremer F: Cerveau "isolé" et physiologie du sommeil. CR Soc Biol (Paris) 1935; 118:1235–41
82. Villablanca J: Electroencephalogram in the permanently isolated forebrain of the cat. Science 1962; 138:44–6. doi:10.1126/science.138.3536.44
83. Steriade M: Arousal: Revisiting the reticular activating system. Science 1996; 272:225–6. doi:10.1126/science.272.5259.225
84. Steriade M, McCormick DA, Sejnowski TJ: Thalamocortical oscillations in the sleeping and aroused brain. Science 1993; 262:679–85. doi:10.1126/science.8235588
85. Torao-Angosto M, Manasanch A, Mattia M, Sanchez-Vives MV: Up and down states during slow oscillations in slow-wave sleep and different levels of anesthesia. Front Syst Neurosci 2021; 15:609645. doi:10.3389/fnsys.2021.609645
86. Lewis LD, Weiner VS, Mukamel EA, et al.: Rapid fragmentation of neuronal networks at the onset of propofol-induced unconsciousness. Proc Natl Acad Sci U S A 2012; 109:E3377–86. doi:10.1073/pnas.1210907109
87. Ní Mhuircheartaigh R, Warnaby C, Rogers R, Jbabdi S, Tracey I: Slow-wave activity saturation and thalamocortical isolation during propofol anesthesia in humans. Sci Transl Med 2013; 5:208ra148. doi:10.1126/scitranslmed.3006007
88. Frohlich J, Toker D, Monti MM: Consciousness among delta waves: A paradox? Brain 2021; 144:2257–77. doi:10.1093/brain/awab095
89. Sanders RD, Mostert N, Lindroth H, Tononi G, Sleigh J: Is consciousness frontal? Two perioperative case reports that challenge that concept. Br J Anaesth 2018; 121:330–2. doi:10.1016/j.bja.2018.01.010
90. Gaskell AL, Hight DF, Winders J, et al.: Frontal alpha-delta EEG does not preclude volitional response during anaesthesia: Prospective cohort study of the isolated forearm technique. Br J Anaesth 2017; 119:664–73. doi:10.1093/bja/aex170
91. Kaplon AW, Gallo S, Guay CS, Baker KH: A black swan spotted during emergence from general anaesthesia: Alpha and delta oscillations present in a conversing patient. Br J Anaesth 2025; 135:1088–90. doi:10.1016/j.bja.2025.06.029
92. Mashour GA, Avidan MS: Black swans: Challenging the relationship of anaesthetic-induced unconsciousness and electroencephalographic oscillations in the frontal cortex. Br J Anaesth 2017; 119:563–5. doi:10.1093/bja/aex207
93. Fultz NE, Bonmassar G, Setsompop K, et al.: Coupled electrophysiological, hemodynamic, and cerebrospinal fluid oscillations in human sleep. Science 2019; 366:628–31. doi:10.1126/science.aax5440
94. Mander BA, Rao V, Lu B, et al.: Prefrontal atrophy, disrupted NREM slow waves and impaired hippocampal-dependent memory in aging. Nat Neurosci 2013; 16:357–64. doi:10.1038/nn.3324
95. Smith SK, Kafashan M, Rios RL, et al.: Daytime dexmedetomidine sedation with closed-loop acoustic stimulation alters slow wave sleep homeostasis in healthy adults. BJA Open 2024; 10:100276. doi:10.1016/j.bjao.2024.100276
96. Kang J, Cho YS, Lee M, et al.: Effects of nonpharmacological interventions on sleep improvement and delirium prevention in critically ill patients: A systematic review and meta-analysis. Aust Crit Care 2023; 36:640–9. doi:10.1016/j.aucc.2022.04.006
97. Luetz A, Grunow JJ, Mörgeli R, et al.: Innovative ICU solutions to prevent and reduce delirium and post-intensive care unit syndrome. Semin Respir Crit Care Med 2019; 40:673–86. doi:10.1055/s-0039-1698404
98. Kafashan MM, Hyche O, Nguyen T, et al.: Perioperative sleep in geriatric cardiac surgical patients: A feasibility study using a wireless wearable device. Br J Anaesth 2021; 126:e205–8. doi:10.1016/j.bja.2021.02.018
99. Guay CS, Labonte AK, Montana MC, et al.: Closed-loop acoustic stimulation during sedation with dexmedetomidine (CLASS-D): Protocol for a within-subject, crossover, controlled, interventional trial with healthy volunteers. Nat Sci Sleep 2021; 13:303–13. doi:10.2147/NSS.S293160

100. Lewis LD, Ching S, Weiner VS, et al.: Local cortical dynamics of burst suppression in the anaesthetized brain. Brain 2013; 136:2727–37. doi:10.1093/brain/awt174
101. Kafashan M, Brian Hickman L, Labonte AK, et al.: Quiescence during burst suppression and postictal generalized EEG suppression are distinct patterns of activity. Clin Neurophysiol 2022; 142:125–32. doi:10.1016/j.clinph.2022.07.493
102. Ching S, Purdon PL, Vijayan S, Kopell NJ, Brown EN: A neurophysiological-metabolic model for burst suppression. Proc Natl Acad Sci U S A 2012; 109:3095–100. doi:10.1073/pnas.1121461109
103. Westover MB, Ching S, Kumaraswamy VM, et al.: The human burst suppression electroencephalogram of deep hypothermia. Clin Neurophysiol 2015; 126:1901–14. doi:10.1016/j.clinph.2014.12.022
104. Werner C, Hoffman WE, Kochs E, Albrecht RF, Schulte am Esch J: Transcranial Doppler sonography indicates critical brain perfusion during hemorrhagic hypotension in dogs. Anesth Analg 1995; 81:1203–7. doi:10.1097/00000539-199512000-00015
105. Schiff ND, Brown EN: Protective down-regulated states in the human brain: A possible lesson from COVID-19. Proc Natl Acad Sci U S A 2022; 119:e2120221119. doi:10.1073/pnas.2120221119
106. Auer RN, Olsson Y, Siesjö BK: Hypoglycemic brain injury in the rat. Correlation of density of brain damage with the EEG isoelectric time: A quantitative study. Diabetes 1984; 33:1090–8. doi:10.2337/diab.33.11.1090
107. Hofmeijer J, Tjepkema-Cloostermans MC, van Putten MJAM: Burst-suppression with identical bursts: A distinct EEG pattern with poor outcome in postanoxic coma. Clin Neurophysiol 2014; 125:947–54. doi:10.1016/j.clinph.2013.10.017
108. Shanker A, Abel JH, Schamberg G, Brown EN: Etiology of burst suppression EEG patterns. Front Psychol 2021; 12:673529. doi:10.3389/fpsyg.2021.673529
109. Zeiler FA, Akoth E, Gillman LM, West M: Burst suppression for ICP control: A systematic review. J Intensive Care Med 2017; 32:130–9. doi:10.1177/0885066615593939
110. Holtkamp M: Pharmacotherapy for refractory and super-refractory status epilepticus in adults. Drugs 2018; 78:307–26. doi:10.1007/s40265-017-0859-1
111. Kajimoto M, Atkinson DB, Ledee DR, et al.: Propofol compared with isoflurane inhibits mitochondrial metabolism in immature swine cerebral cortex. J Cereb Blood Flow Metab 2014; 34:514–21. doi:10.1038/jcbfm.2013.229
112. Vanlander AV, Okun JG, de Jaeger A, et al.: Possible pathogenic mechanism of propofol infusion syndrome involves coenzyme q. Anesthesiology 2015; 122:343–52. doi:10.1097/ALN.0000000000000484
113. He L, Wang X, Zheng S: Inhibition of the electron transport chain in propofol induced neurotoxicity in zebrafish embryos. Neurotoxicol Teratol 2020; 78:106856. doi:10.1016/j.ntt.2020.106856
114. Voss LJ, Sleigh JW: A metabolic mechanism for anaesthetic suppression of cortical synaptic function in mouse brain slices-A pilot investigation. Int J Mol Sci 2020; 21:4703. doi:10.3390/ijms21134703
115. Berndt N, Rösner J, Haq RU, et al.: Possible neurotoxicity of the anesthetic propofol: Evidence for the inhibition of complex II of the respiratory chain in area CA3 of rat hippocampal slices. Arch Toxicol 2018; 92:3191–205. doi:10.1007/s00204-018-2295-8
116. Frohlich J, Johnson MA, McArthur DL, et al.: Sedation-induced burst suppression predicts positive outcome following traumatic brain injury. Front Neurol 2021; 12:750667. doi:10.3389/fneur.2021.750667
117. Watson PL, Shintani AK, Tyson R, Pandharipande PP, Pun BT, Ely EW: Presence of electroencephalogram burst suppression in sedated, critically ill patients is associated with increased mortality. Crit Care Med 2008; 36:3171–7. doi:10.1097/CCM.0b013e318186b9ce
118. Hogan J, Sun H, Aboul Nour H, et al.: Burst suppression: Causes and effects on mortality in critical illness. Neurocrit Care 2020; 33:565–74. doi:10.1007/s12028-020-00932-4
119. Pedemonte JC, Plummer GS, Chamadia S, et al.: Electroencephalogram burst-suppression during cardiopulmonary bypass in elderly patients mediates postoperative delirium. Anesthesiology 2020; 133:280–92. doi:10.1097/ALN.0000000000003328
120. Andresen JM, Girard TD, Pandharipande PP, Davidson MA, Ely EW, Watson PL: Burst suppression on processed electroencephalography as a predictor of postcoma delirium in mechanically ventilated ICU patients. Crit Care Med 2014; 42:2244–51. doi:10.1097/CCM.0000000000000522
121. Sessler DI, Sigl JC, Kelley SD, et al.: Hospital stay and mortality are increased in patients having a "triple low" of low blood pressure, low Bispectral Index, and low minimum alveolar concentration of volatile anesthesia. Anesthesiology 2012; 116:1195–203. doi:10.1097/ALN.0b013e31825683dc
122. Willingham MD, Karren E, Shanks AM, et al.: Concurrence of intraoperative hypotension, low minimum alveolar concentration, and low Bispectral Index is associated with postoperative death. Anesthesiology 2015; 123:775–85. doi:10.1097/ALN.0000000000000822
123. Fernandes JA, Lutz PL, Tannenbaum A, Todorov AT, Liebovitch L, Vertes R: Electroencephalogram activity in the anoxic turtle brain. Am J Physiol 1997; 273:R911–9. doi:10.1152/ajpregu.1997.273.3.R911

124. Johnson KB, Egan TD, Kern SE, et al.: The influence of hemorrhagic shock on propofol: A pharmacokinetic and pharmacodynamic analysis. Anesthesiology 2003; 99:409–20. doi:10.1097/00000542-200308000-00023
125. Johnson KB, Egan TD, Kern SE, McJames SW, Cluff ML, Pace NL: Influence of hemorrhagic shock followed by crystalloid resuscitation on propofol: A pharmacokinetic and pharmacodynamic analysis. Anesthesiology 2004; 101:647–59. doi:10.1097/00000542-200409000-00013
126. Kurita T, Takata K, Morita K, et al.: The influence of hemorrhagic shock on the electroencephalographic and immobilizing effects of propofol in a swine model. Anesth Analg 2009; 109:398–404. doi:10.1213/ane.0b013e3181a96f9a
127. Georgii M-T, Kreuzer M, Fleischmann A, Schuessler J, Schneider G, Pilge S: Targeted interventions to increase blood pressure and decrease anaesthetic concentrations reduce intraoperative burst suppression: A randomised, interventional clinical trial. Front Syst Neurosci 2022; 16:786816. doi:10.3389/fnsys.2022.786816
128. Zhou DW, Westover MB, McClain LM, et al.: Clustering analysis to identify distinct spectral components of encephalogram burst suppression in critically ill patients. Annu Int Conf IEEE Eng Med Biol Soc 2015; 2015:7258–61. doi:10.1109/EMBC.2015.7320067
129. Jones KG, Lybbert C, Euler MJ, et al.: Diversity of electroencephalographic patterns during propofol-induced burst suppression. Front Syst Neurosci 2023; 17:1172856. doi:10.3389/fnsys.2023.1172856
130 Fleischmann A, Pilge S, Kiel T, Kratzer S, Schneider G, Kreuzer M: Substance-specific differences in human electroencephalographic burst suppression patterns. Front Hum Neurosci 2018; 12:368. doi:10.3389/fnhum.2018.00368
131. Mink JW, Blumenschine RJ, Adams DB: Ratio of central nervous system to body metabolism in vertebrates: Its constancy and functional basis. Am J Physiol 1981; 241:R203–12. doi:10.1152/ajpregu.1981.241.3.R203
132. Harris JJ, Jolivet R, Attwell D: Synaptic energy use and supply. Neuron 2012; 75:762–77. doi:10.1016/j.neuron.2012.08.019
133. Attwell D, Laughlin SB: An energy budget for signaling in the grey matter of the brain. J Cereb Blood Flow Metab 2001; 21:1133–45. doi:10.1097/00004647-200110000-00001
134. Marshall M, Longley BP, Stanton WH: Electroencephalography in anaesthetic practice. Br J Anaesth 1965; 37:845–57. doi:10.1093/bja/37.11.845
135. Wei W, Song Y, Fan X, et al.: Simultaneous recording of brain extracellular glucose, spike and local field potential in real time using an implantable microelectrode array with nano-materials. Nanotechnology 2016; 27:114001. doi:10.1088/0957-4484/27/11/114001
136. Yan TD, Bannon PG, Bavaria J, et al.: Consensus on hypothermia in aortic arch surgery. Ann Cardiothorac Surg 2013; 2:163–8. doi:10.3978/j.issn.2225-319X.2013.03.03
137. Michenfelder JD, Milde JH: The relationship among canine brain temperature, metabolism, and function during hypothermia. Anesthesiology 1991; 75:130–6. doi:10.1097/00000542-199107000-00021
138. Myers RR, Stockard JJ, Saidman LJ: Monitoring of cerebral perfusion during anesthesia by time-compressed Fourier analysis of the electroencephalogram. Stroke 1977; 8:331–7. doi:10.1161/01.str.8.3.331
139. Gavilanes AW, Vles JS, von Siebenthal K, et al.: Electrocortical brain activity, cerebral haemodynamics and oxygenation during progressive hypotension in newborn piglets. Clin Neurophysiol 2001; 112:52–9. doi:10.1016/s1388-2457(00)00499-5
140. Kamitaki BK, Tu B, Wong S, Mendiratta A, Choi H: Quantitative EEG changes correlate with post-clamp ischemia during carotid endarterectomy. J Clin Neurophysiol 2021; 38:213–20. doi:10.1097/WNP.0000000000000686
141. Budzinska K, Ilasz R: Electroencephalographic and respiratory activities during acute intermittent hypoxia in anesthetized rats. J Physiol Pharmacol 2007; 58:85–93
142. Brechner VL, Kinnell J, Bauer RO, Bethune RW, Dillon J: electroencephalographic signs of HYPOXIA in the anesthetized dog. Anesth Analg 1965; 44:320–6
143. Wong NY, van Waart H, Sleigh JW, Mitchell SJ, Vrijdag XC: A systematic review of electroencephalography in acute cerebral hypoxia: Clinical and diving implications. Diving Hyperb Med 2023; 53:268–80. doi:10.28920/dhm53.3.268-280
144. Meyer JS, Sakamoto K, Akiyama M, Yoshida K, Yoshitake S: Monitoring cerebral blood flow, metabolism and EEG. Electroencephalogr Clin Neurophysiol 1967; 23:497–508 10.1016/0013-4694(67)90016-8
145. Sánchez Fustes A, Reinoso Barbero F, Elvira Lafuente C, Torres Maestro B, Burgos Morales P, González Pizarro P: Electroencephalographic findings during transfusion therapy throughout emergent ECMO cannulation in a refractory respiratory failure infant with tetralogy of Fallot: A case report. J Clin Monit Comput 2024; 38:1219–23. doi:10.1007/s10877-024-01169-8
146. Morimoto Y, Mathru M, Martinez-Tica JF, Zornow MH: Effects of profound anemia on brain tissue oxygen tension, carbon dioxide tension, and pH in rabbits. J Neurosurg Anesthesiol 2001; 13:33–9. doi:10.1097/00008506-200101000-00006

147. Blaabjerg L, Juhl CB: Hypoglycemia-induced changes in the electroencephalogram: An overview. J Diabetes Sci Technol 2016; 10:1259–67. doi:10.1177/1932296816659744
148. Sharbrough FW, Messick JM Jr, Sundt TM Jr: Correlation of continuous electroencephalograms with cerebral blood flow measurements during carotid endarterectomy. Stroke 1973; 4:674–83. doi:10.1161/01.str.4.4.674
149. Smith AL, Wollman H: Cerebral blood flow and metabolism: Effects of anesthetic drugs and techniques. Anesthesiology 1972; 36:378–400. doi:10.1097/00000542-197204000-00015
150. Foreman B, Claassen J: Quantitative EEG for the detection of brain ischemia. Crit Care 2012; 16:216. doi:10.1186/cc11230
151. Stepanek J, Dunn RA, Pradhan GN, Cevette MJ: Supplemental CO2 improves oxygen saturation, oxygen tension, and cerebral oxygenation in acutely hypoxic healthy subjects. Physiol Rep 2020; 8:e14513. doi:10.14814/phy2.14513
152. Hoiland RL, Bain AR, Rieger MG, Bailey DM, Ainslie PN: Hypoxemia, oxygen content, and the regulation of cerebral blood flow. Am J Physiol Regul Integr Comp Physiol 2016; 310:R398–413. doi:10.1152/ajpregu.00270.2015
153. Ainslie PN, Ogoh S: Regulation of cerebral blood flow in mammals during chronic hypoxia: A matter of balance: Hypoxia-induced regulation of cerebral perfusion. Exp Physiol 2010; 95:251–62. doi:10.1113/expphysiol.2008.045575
154. Yamashiro SM, Kato T: Modeling cerebral blood flow and ventilation instability due to CO2. J Appl Physiol (1985) 2021; 130:1427–35. doi:10.1152/japplphysiol.00949.2020
155. Vu EL, Brown CH 4th, Brady KM, Hogue CW: Monitoring of cerebral blood flow autoregulation: Physiologic basis, measurement, and clinical implications. Br J Anaesth 2024; 132:1260–73. doi:10.1016/j.bja.2024.01.043
156. Croughwell N, Smith LR, Quill T, et al.: The effect of temperature on cerebral metabolism and blood flow in adults during cardiopulmonary bypass. J Thorac Cardiovasc Surg 1992; 103:549–54
157. Reves JG: Toward understanding cerebral blood flow during cardiopulmonary bypass: Implications for the central nervous system. Anesthesiology 2019; 130:609–13. doi:10.1097/ALN.0000000000002580
158. Nakano M, Nomura Y, Whitman G, et al.: Cerebral autoregulation in the operating room and intensive care unit after cardiac surgery. Br J Anaesth 2021; 126:967–74. doi:10.1016/j.bja.2020.12.043
159. Massari D, de Keijzer IN, Scheeren TWL: Cerebral monitoring in surgical ICU patients. Curr Opin Crit Care 2021; 27:701–8. doi:10.1097/MCC.0000000000000871
160. Smith SM, Padayachee S, Modaresi KB, Smithies MN, Bihari DJ: Cerebral blood flow is proportional to cardiac index in patients with septic shock. J Crit Care 1998; 13:104–9. doi:10.1016/s0883-9441(98)90013-2
161. Sasaoka K, Ohta H, Ishizuka T, Kojima K, Sasaki N, Takiguchi M: Transcranial Doppler ultrasonography detects the elevation of cerebral blood flow during ictal-phase of pentetrazol-induced seizures in dogs. Am J Vet Res 2022; 83:331–8. doi:10.2460/ajvr.21.06.0085
162. Yoshida H, Kushikata T, Kabara S, Takase H, Ishihara H, Hirota K: Flat electroencephalogram caused by carbon dioxide pneumoperitoneum. Anesth Analg 2007; 105:1749–52, table of contents. doi:10.1213/01.ane.0000290293.13532.60
163. Eisele JH, Eger EI 2nd, Muallem M: Narcotic properties of carbon dioxide in the dog. Anesthesiology 1967; 28:856–65. doi:10.1097/00000542-196709000-00019
164. Wang D, Yee BJ, Wong KK, et al.: Comparing the effect of hypercapnia and hypoxia on the electroencephalogram during wakefulness. Clin Neurophysiol 2015; 126:103–9. doi:10.1016/j.clinph.2014.04.012
165. Weeke LC, Dix LML, Groenendaal F, et al.: Severe hypercapnia causes reversible depression of aEEG background activity in neonates: An observational study. Arch Dis Child Fetal Neonatal Ed 2017; 102:F383–8. doi:10.1136/archdischild-2016-311770
166. Reshef ER, Schiff ND, Brown EN: A neurologic examination for anesthesiologists: Assessing arousal level during induction, maintenance, and emergence. Anesthesiology 2019; 130:462–71. doi:10.1097/ALN.0000000000002559
167. Sessler CN, Gosnell MS, Grap MJ, et al.: The Richmond Agitation-Sedation Scale: Validity and reliability in adult intensive care unit patients. Am J Respir Crit Care Med 2002; 166:1338–44. doi:10.1164/rccm.2107138
168. Roustan J-P, Valette S, Aubas P, Rondouin G, Capdevila X: Can electroencephalographic analysis be used to determine sedation levels in critically ill patients? Anesth Analg 2005; 101:1141–51. doi:10.1213/01.ane.0000167782.47957.e1
169. Vacas S, McInrue E, Gropper MA, et al.: The feasibility and utility of continuous sleep monitoring in critically ill patients using a portable electroencephalography monitor. Anesth Analg 2016; 123:206–12. doi:10.1213/ANE.0000000000001330
170. Prerau MJ, Brown RE, Bianchi MT, Ellenbogen JM, Purdon PL: Sleep neurophysiological dynamics through the lens of multitaper

spectral analysis. Physiology (Bethesda) 2017; 32:60–92. doi:10.1152/physiol.00062.2015
171. Hight DF, Kaiser HA, Sleigh JW, Avidan MS: Continuing professional development module: An updated introduction to electroencephalogram-based brain monitoring during intended general anesthesia. Can J Anaesth 2020; 67:1858–78. doi:10.1007/s12630-020-01820-3
172. Piva S, Bertoni M, Gitti N, Rasulo FA, Latronico N: Neurological complications of sepsis. Curr Opin Crit Care 2023; 29:75–84. doi:10.1097/MCC.0000000000001022
173. Gofton TE, Young GB: Sepsis-associated encephalopathy. Nat Rev Neurol 2012; 8:557–66. doi:10.1038/nrneurol.2012.183
174. Young GB, Bolton CF, Archibald YM, Austin TW, Wells GA: The electroencephalogram in sepsis-associated encephalopathy. J Clin Neurophysiol 1992; 9:145–52. doi:10.1097/00004691-199201000-00016
175. Oddo M, Carrera E, Claassen J, Mayer SA, Hirsch LJ: Continuous electroencephalography in the medical intensive care unit. Crit Care Med 2009; 37:2051–6. doi:10.1097/CCM.0b013e3181a00604
176. Brown EN, Pavone KJ, Naranjo M: Multimodal general anesthesia: Theory and practice. Anesth Analg 2018; 127:1246–58. doi:10.1213/ANE.0000000000003668
177. Couture EJ, Deschamps A, Denault AY: Patient management algorithm combining processed electroencephalographic monitoring with cerebral and somatic near-infrared spectroscopy: A case series. Can J Anaesth 2019; 66:532–9. doi:10.1007/s12630-019-01305-y
178. Guay CS, Avidan MS: No brain is an island. Anesth Analg 2020; 130:1568–71. doi:10.1213/ANE.0000000000004704